

Vortical waves in a quantum fluid with vector, axial and helical charges. I. Non-dissipative transport

Sergio Morales-Tejera,^a Victor E. Ambruş^{1a} and Maxim N. Chernodub^{2b,a}

^a*Department of Physics, West University of Timișoara,
Bd. Vasile Pârvan 4, Timișoara 300223, Romania*

^b*Institut Denis Poisson, Université de Tours, Tours 37200, France*

E-mail: sergio.morales@e-uvt.ro, victor.ambrus@e-uvt.ro,
maxim.chernodub@univ-tours.fr

ABSTRACT: Due to the spin-orbit coupling, Dirac fermions, submerged in a thermal bath with finite macroscopic vorticity, exhibit a spin polarisation along the direction parallel to the vorticity vector Ω . Due to the symmetries of the Lagrangian for free massless Dirac particles, there are three independent and classically conserved currents corresponding to the vector, axial, and helical charges. The constitutive relations for the charge currents and the stress-energy tensor at thermal equilibrium, derived in the framework of quantum field theory at finite temperature, reveal vorticity-induced contributions that deviate from the perfect fluid form. In this paper, we consider the mode structure of the corresponding hydrodynamical theory and derive collective excitations associated with coherent fluctuations of all three charges. We show that the chirally imbalanced rotating fluid should possess non-reciprocal gapless waves that propagate with different velocities along and opposite to the vorticity vector. We also uncover a strictly unidirectional mode, which we call the Axial Vortical Wave, propagating in the background of the axial charge density. We point out an unexpected instability in the limit of degenerate matter and discuss possible solutions when helicity and axial charge non-conservation is taken into account.

¹Corresponding author.

²Corresponding author.

Contents

1	Introduction	1
2	Anomalous transport in vortical fluids	5
2.1	Quantum vortical effects	5
2.2	The Landau frame	7
2.3	Vector/axial/helical anomalous vortical transport as spin-orbit coupling	8
2.4	Conservation equations for longitudinal perturbations	12
2.5	Full space-time solutions from Fourier modes	15
3	Hydrodynamic waves at high temperature	17
3.1	Helical Vortical Wave	19
3.2	Axial Vortical Wave	21
3.3	Propagation properties	23
3.4	Symmetries of the helical and axial vortical waves	24
4	Unpolarized Plasma	26
5	Degenerate limit of high-density matter and non-reciprocity	30
6	Summary and Conclusions	35

1 Introduction

Chiral fluids possess a class of hydrodynamic gapless excitations that emerge due to a coherent interplay of appropriate channels in the transfer and accumulation of (approximately) conserved charges of the system [1–3]. These hydrodynamic modes appear in the electromagnetic field background and curved (notably, vortical) spacetimes. They are distinguished from other excitations because their very existence is supported by the anomalous breaking of continuous internal symmetries in the system, such as the chiral anomaly or the mixed gauge-gravitational anomaly (for an extensive review, see Ref. [4]).

The Chiral Magnetic Wave [1] represents a neat example of an anomalous hydrodynamic mode. This excitation is supported by two transport phenomena, both arising due to the axial anomaly: the Chiral Magnetic Effect [5–7] and the Chiral Separation Effect [8, 9]. The first phenomenon generates a vector current in a region with a nonvanishing chiral charge density. This current, directed along the axis of the background magnetic field, leads to a vector charge accumulation, which serves, in turn, as a source for the chiral current generated now by the second effect. The chiral current transports the chiral charge further along the magnetic field axis, and the process repeats cyclically again, producing the Chiral Magnetic Wave excitation in the vector and axial charge densities of chiral fermions.

The Chiral Magnetic Wave was hypothesized to emerge in the quark-gluon plasma that possibly has certain experimental signatures [10]. A similar excitation also appears in the vortical backgrounds via chiral vortical effects [11, 12], which produce intertwining fluctuations of vector and axial currents and their charges along the axis of rotation [2].

In the standard picture described above, the chiral fluids are traditionally described as two-component systems that incorporate vector and axial charges and their currents. However, in addition to these local quantities, ensembles of massless fermions also possess a third class of charges and currents associated with the helicity of massless fermions (see a detailed pedagogical discussion in Ref. [13] along with a more recent account in [14, 15]). In a generic ensemble of fermions, helicity enters as an independent local characteristic of the ensemble, which is distinct from the vector (electric) and axial (chiral) charges.

Our paper intensively explores the role of the helical degrees of freedom in the hydrodynamic context of vortical chiral fluids. The spectrum of the hydrodynamic modes in rotating fluids contains a multitude of hydrodynamical gapless excitations, even if the helical degree of freedom is not accounted for [1–3, 16–22]. The main aim of the work is to identify the physical consequences of the correct incorporation of the helicity property, which must be present in a system possessing more than one chiral fermion, for the hydrodynamics of these fluids. In this paper, we work in the dissipationless limit, when both the axial and helical quantum numbers are strictly conserved.

Helicity is often confusingly identified with chirality, even though these two properties reflect separate physical features of fermions. Its precise nature is highlighted by the simple observation that the chirality property equally applies to particles and anti-particles, while the helicity distinguishes between them. The critical distinction, often misunderstood, lies in the fact that a fermion’s chirality matches its helicity, whereas an anti-fermion’s chirality is opposite to its helicity. This difference leads to an incorrect generalization, “chirality equals helicity,” which does not hold in many-body particle-antiparticle systems. For instance, a fermion–anti-fermion pair can have either combined chirality and zero helicity (if their chiralities align) or zero total chirality but non-zero helicity (if their chiralities are opposite). This striking dissimilarity between chirality and helicity can also be emphasized by the difference in their charge conjugation symmetries: while the chiral charge density is a C -even quantity, its helical counterpart has a C -odd symmetry with respect to the charge conjugation [14, 15].

The distinct nature of the vector, chiral, and helical quantum numbers is highlighted by the following relation between the charges of an individual massless (anti-)fermion:

$$q_V q_A = q_H, \quad q_A q_H = q_V, \quad q_H q_V = q_A, \quad q_V q_A q_H = 1, \quad (1.1)$$

where the vector charge q_V discriminates a particle ($q_V = +1$) from an anti-particle ($q_V = -1$), the helical charge q_H labels the relative orientation of the momentum and spin directions, distinguishing parallel vectors ($q_H = +1$) and antiparallel vectors ($q_H = -1$), while the last entry in the triad, the chiral charge q_A , shows that the chirality for a particle (anti-particle) coincides with (is opposite to) its helicity q_H . The relation (1.1) links tightly the helicity and chirality for a single massless (anti-)particle. However, it is not generally

valid for a system of massless fermions, therefore making the total helicity charge of an ensemble disconnected from the total chiral charge of the same ensemble. Thus, the helicity becomes an independent degree of freedom of the system, distinct from chirality. The similarities and differences between chiral and helical degrees of freedom, already emphasised by Eq. (1.1), are illustrated in detail in Fig. 1, discussed in Sec. 2.3, where the origin of Chiral and Helical Vortical Effects is demonstrated in a simple pictorial form based on a straightforward counting of the vector, axial, and helical degrees of freedom.

In addition, one may argue that the helical degree of freedom is as good (bad) as the chiral charge of massive fermions: neither of them is conserved in physically relevant theories such as massive QED or QCD. In the relaxation time approximation, the pertinence of these quantum numbers for the dynamics of the system is determined by the relative order of magnitudes of the axial, τ_A , and helical, τ_H , relaxation times, which show how fast these charges dissolve in the system. Similarly to the axial (chiral) charge [23, 24], the relaxation of the helical charge might also be a rather fast process [25]. In addition to the charge relaxation times, the system is also characterized by the kinetic relaxation time τ_R , which encodes how fast fluctuations in the thermodynamic characteristics of the system (such as pressure and energy density) relax towards the thermodynamic equilibrium. In general, all three relaxation times, τ_R , τ_A , and τ_H , are independent of each other. We defer the discussion of the consequences of these dissipative effects to the paper representing the second part of this work [26]. In this first part, we will focus on exploring the wide spectrum of coherent excitations that develop at the level of the vector, axial and helicity currents at both large and small temperatures, with or without background axial or helical imbalance.

In this paper, we concentrate on helicity-catalyzed waves that emerge in the rotating, also called vortical, fluids. While certain properties of gapless hydrodynamic excitations in the magnetic background field were already analyzed in Ref. [27], the vortical background represents a more attractive perspective from the point of view of the experimental verification of these effects in relativistic heavy-ion collisions. Here, the vorticity refers to the local angular momentum or rotational motion of the quark-gluon plasma (QGP), which is generated in a highly vortical state due to the angular momentum conservation and the initial asymmetry in the non-central collision geometry [28].

While both vorticity and magnetic fields are generated almost simultaneously during the collision, the key difference between them is their lifetime. Magnetic field decays very rapidly as the expanding plasma cannot maintain it due to relatively low electrical conductivity [29–31]. In contrast, the vorticity, once established in the QGP, is sustained due to the mechanical conservation of the angular momentum [28]. The emergence of vorticity can be inferred from the spin polarization of emitted particles [32–34], which is a measure of the alignment of their spins with the (local or global) angular momentum of the QGP [35, 36].

The hydrodynamic wave excitations that emerge in vortical plasmas of chiral fermions propagate along the vorticity vector in the plasma. They can leave experimental signatures that resemble the Chiral Magnetic Wave, imprinted, supposedly, in other observables. Below, we concentrate on the theoretical questions related to the very existence of these modes, their spectrum, and their lifetimes. The discussion of their experimental signatures will be presented elsewhere.

In our paper, we stress that the incorporation of the helical charges is important for the hydrodynamics of the system. In particular, in a system of rotating Dirac fermions at finite temperature and density, the accounting of the helical degree of freedom drastically affects the hydrodynamic spectrum. For example, a new type of excitations, suggested under a collective name “the helical vortical effects,” emerges as hydrodynamic modes that intertwine coherent fluctuations of vector, axial, and helical charges [15]. At the typical parameters of the quark-gluon plasma, the helical modes show a rather profound difference compared to chiral modes, implying, in particular, that the Helical Vortical Wave propagates much faster than the Chiral Vortical Wave [15]. Notice that the Chiral and Helical Vortical Waves and their generalization, considered in this paper, should be distinguished from the chiral density wave [37] and its dual analogue [38] (also, in rotating matter [39, 40]) that emerge in the dense matter and are characterized by a static coherent state of spatially varying scalar and pseudoscalar condensates.

We will also show below that in the presence of a non-vanishing axial (chiral) chemical potential, the system of massless fermions hosts the Axial Vortical Wave (AVW). On a background with positive (negative) chiral imbalance, this rather unusual excitation propagates only opposite to (along) the vector of vorticity and not forward (backwards). Notice that the existence of the AVW does not rely on helical degrees of freedom, as this excitation can also propagate in the purely axial sector. The non-reciprocity of wave propagation is a remarkable and relatively rare phenomenon that needs a particular set of conditions. For example, in the condensed matter setting, one can find a unidirectional propagation of phonons associated with longitudinal vibrations of a twisted crystal lattice of Weyl semimetals that exhibit the axial anomaly [41]. The phonons propagate only along the direction of the twist and not backward. This excitation, dubbed the chiral sound wave, resembles the Axial Vortical Wave because the twist of the crystal can be associated with the vorticity of the underlying ion lattice.

The structure of the paper is as follows. In Sec. 2, we describe the rotating state in thermal equilibrium. We then formulate the equations obeyed by the fluctuations around this state in the Landau frame in the vicinity of the rotation axis. In our setup, the fluctuations of the charge sector decouple from the energy-momentum sector in the Landau frame.

As already mentioned above, in this work, we analyze the wave spectrum arising in a rotating V/A/H fluid when all three charges are conserved. In Sec. 3, we discuss the wave spectrum in the large temperature limit. The emergence of the Helical Vortical Wave and the strictly unidirectional Axial Vortical Wave is demonstrated in Subsections 3.1 and 3.2. We discuss the case of an unpolarized plasma in Subsec. 4, where the axial and the helical chemical potentials vanish, which can be treated exactly to a high degree. In Sec. 5, we discuss the so-called degenerate limit when the vector chemical potential μ_V is larger than the temperature and the other chemical potentials. This case—which can be dubbed as a weakly polarized plasma—corresponds to a realistic high-density matter state ($|\mu_V| \gg T$). At the same time, the smallness of the other chemical potentials (μ_A and μ_H) emulates the non-conservation of the corresponding charges.

2 Anomalous transport in vortical fluids

We start this section with a brief review of the vortical effects involving the thermal expectation values of the energy-momentum tensor and of the vector, axial and helicity currents, summarized in Subsec. 2.1. We then discuss the transition from the natural thermometer (β) frame to the Landau frame in the limit of slow rotation in Subsec. 2.2. Then, we consider the conservation properties of the vortical/axial/helical ($V/A/H$, for shortness) currents considered in this paper. We leave a discussion of the mechanisms leading to their non-conservation in the companion paper [26]. Finally, we present the general framework for the analysis of vortical waves in Subsec. 2.4.

2.1 Quantum vortical effects

Due to spin-orbit coupling, a fermionic plasma under rotation develops a spin polarization current along the direction of the local vorticity vector. More specifically, let us consider free massless fermions, described by the Dirac Lagrangian $\mathcal{L} = i\bar{\psi}\not{\partial}\psi$. These fermions may be characterized by their vector charge, distinguishing between particles and anti-particles ($\sigma = \pm 1$), axial charge ($\xi = \pm 1$), and helical charge ($\lambda = \pm 1/2$). Rotating states may be described in the grand canonical ensemble using the density operator

$$\hat{\rho} = \exp \left[-\beta(\hat{H} - \Omega\hat{J}^z - \vec{\mu} \cdot \hat{\vec{Q}}) \right], \quad (2.1)$$

where \hat{H} and \hat{J}^z are the system's Hamiltonian and z -axis total angular momentum, while $\hat{\vec{Q}} = (\hat{Q}_V, \hat{Q}_A, \hat{Q}_H)$ collectively denotes the vector, axial and helical charge operators, respectively. The Lagrange multipliers β , Ω and $\vec{\mu} = (\mu_V, \mu_A, \mu_H)$ corresponding to these (conserved) operators characterize the system inverse temperature, angular velocity, and vector/axial/helical chemical potentials, respectively. The statistical operator (2.1) defines a preferred frame, called the thermometer (or β) frame, characterized by the four-velocity corresponding to rigid rotation:

$$u_\Omega^\mu \partial_\mu = \Gamma_\Omega(\partial_t + \Omega\partial_\varphi), \quad \Gamma_\Omega = \frac{1}{\sqrt{1 - \rho^2\Omega^2}}, \quad (2.2)$$

where (t, ρ, φ, z) represent cylindrical coordinates and ρ is the transverse-plane distance to the rotation axis z . The velocity profile in Eq. (2.2) allows one to introduce a so-called kinematic tetrad, comprised of the four-velocity u^μ , the kinematic vorticity vector $\omega^\mu = \frac{1}{2}\varepsilon^{\mu\nu\lambda\sigma}u_\nu\nabla_\lambda u_\sigma$, acceleration vector $a^\mu = u^\nu\nabla_\nu u^\mu$, as well as a fourth vector $\tau^\mu = -\varepsilon^{\mu\nu\lambda\sigma}\omega_\nu a_\lambda u_\sigma$. In the case of rigid rotation, these four vectors are mutually orthogonal. Explicitly, u^μ is given in Eq. (2.2), while the other three vectors are given as follows:

$$\omega_\Omega = \Omega\Gamma_\Omega^2\partial_z, \quad a_\Omega = -\rho\Omega^2\Gamma_\Omega^2\partial_\rho, \quad \tau_\Omega = -\rho\Omega^3\Gamma_\Omega^5(\rho\Omega\partial_t + \rho^{-1}\partial_\varphi). \quad (2.3)$$

In the classical Dirac theory, the energy-momentum tensor $T^{\mu\nu}$ and the charge currents $J_{V/A/H}^\mu$ read

$$T^{\mu\nu} = \frac{i}{2}\bar{\psi}\gamma^{(\mu}\partial^{\nu)}\psi, \quad J_V^\mu = \bar{\psi}\gamma^\mu\psi, \quad J_A^\mu = \bar{\psi}\gamma^\mu\gamma^5\psi, \quad J_H^\mu = \bar{\psi}\gamma^\mu h\psi + \bar{h}\psi\gamma^\mu\psi. \quad (2.4)$$

In thermal field theory, one may compute the thermal expectation value of an operator \widehat{A} via $A = \langle \widehat{A} \rangle \equiv Z^{-1} \text{tr}(\widehat{\rho} \widehat{A})$, where $Z = \text{tr}(\widehat{\rho})$ is the partition function. The expectation values $T^{\mu\nu} \equiv \langle \widehat{T}^{\mu\nu} \rangle$ and $J_\ell^\mu = \langle \widehat{J}_\ell^\mu \rangle$ of, respectively, the energy-momentum tensor and the charge currents can be obtained in quantum field theory [42–44]. As is customary in relativistic fluid dynamics, one can decompose these quantities uniquely after defining a so-called hydrodynamic frame that fixes the fluid’s four-velocity. In the β frame, the four-velocity is given by u_Ω^μ and

$$J_\ell^\mu = Q_{\ell;\beta} u_\Omega^\mu + V_{\ell;\beta}^\mu, \quad T^{\mu\nu} = E_\beta u_\Omega^\mu u_\Omega^\nu - (P_\beta + \varpi_\beta) \Delta_\Omega^{\mu\nu} + \pi_\beta^{\mu\nu} + W_\beta^\mu u_\Omega^\nu + W_\beta^\nu u_\Omega^\mu, \quad (2.5)$$

where the subscript β reminds us that all quantities appearing on the right-hand sides of the above relations are computed in the β frame. The charge densities $Q_{\ell;\beta}$ ($\ell \in \{V, A, H\}$), energy density E_β and thermodynamic pressure P_β are terms characteristic of a perfect fluid.

In Eq. (2.5), the tensor $\Delta_\Omega^{\mu\nu} = g^{\mu\nu} - u_\Omega^\mu u_\Omega^\nu$ is a projector on the hypersurface orthogonal to u_Ω^μ , while the deviations from the perfect fluid form, namely ϖ_β , $V_{\ell;\beta}^\mu$, W_β^μ and $\pi_\beta^{\mu\nu}$, are by construction traceless and orthogonal to u_Ω^μ . These terms arise as quantum corrections induced by the local acceleration and vorticity of the fluid. For a conformal fluid, the equation of state $E_\beta = 3P_\beta$ and the tracelessness condition $T^\mu{}_\mu = 0$ imply that the dynamic pressure vanishes, $\varpi_\beta = 0$. The constitutive equations for $V_{\ell;\beta}^\mu$, W_β^μ and $\pi_\beta^{\mu\nu}$ in the β frame are given by the vortical effects derived in Ref. [45]:

$$\begin{aligned} V_{\ell;\beta}^\mu &= \sigma_{\ell;\beta}^\omega \omega_\Omega^\mu + \sigma_{\ell;\beta}^\tau \tau_\Omega^\mu, & W_\beta^\mu &= \sigma_{\varepsilon;\beta}^\omega \omega_\Omega^\mu + \sigma_{\varepsilon;\beta}^\tau \tau_\Omega^\mu, \\ \pi_\beta^{\mu\nu} &= \pi_{1;\beta} \left(\tau_\Omega^\mu \tau_\Omega^\nu - \frac{\omega_\Omega^2}{2} a_\Omega^\mu a_\Omega^\nu - \frac{\mathbf{a}_\Omega^2}{2} \omega_\Omega^\mu \omega_\Omega^\nu \right) + \pi_{2;\beta} (\omega_\Omega^\mu \tau_\Omega^\nu + \omega_\Omega^\nu \tau_\Omega^\mu), \end{aligned} \quad (2.6)$$

where $\sigma_{\ell;\beta}^\omega = (\sigma_{V;\beta}^\omega, \sigma_{A;\beta}^\omega, \sigma_{H;\beta}^\omega)$ represent the vector/axial/helical vortical conductivities and $\sigma_{\varepsilon;\beta}^\omega$ is the vortical heat conductivity. Likewise, $\sigma_{\ell;\beta}^\tau$ and $\sigma_{\varepsilon;\beta}^\tau$ represent circular conductivities. Finally, $\pi_{1;\beta}$ and $\pi_{2;\beta}$ represent shear-stress coefficients.

All of the above scalar functions can be calculated in quantum field theory as the sum of a classical term followed by quantum corrections, with the latter being at least quadratic in $\hbar\Omega$. As pointed out in Ref. [45], the classical pressure can be calculated on the basis of an ensemble of polarized fermions described by the Fermi-Dirac distribution,

$$f_{\mathbf{p},\lambda}^{\text{eq};\sigma} = \left[\exp \left(\frac{p \cdot u - \mu_{\sigma,\lambda}}{T} \right) + 1 \right]^{-1}, \quad (2.7)$$

where $p^\mu = (p^0, \mathbf{p})$ is the particle four-momentum ($p^0 = |\mathbf{p}|$ for massless fermions), $\sigma = \pm 1$ distinguishes between particles and anti-particles, while $\lambda = \pm 1/2$ labels the particle helicity. The chemical potential $\mu_{\sigma,\lambda}$ arises due to the vector, axial, and helical imbalances in the system, having the expression

$$\mu_{\sigma,\lambda} = \vec{q}_{\sigma,\lambda} \cdot \vec{\mu} = \sigma \mu_V + 2\lambda \mu_A + 2\sigma \lambda \mu_H, \quad (2.8)$$

where $\vec{q}_{\sigma,\lambda} = \{\sigma, 2\lambda, 2\lambda\sigma\}$ collects the vector, axial and helical charges. In Eq. (2.7), T and $\mu_{\sigma,\lambda}$ represent the local temperature and a set of chemical potentials, respectively.

For example, for the rigidly-rotating system, when $u^\mu \rightarrow u_\Omega^\mu$, temperature T and chemical potentials $\mu_{\sigma,\lambda}$ are given by the Tolman-Ehrenfest law,

$$T = \Gamma_\Omega T_0, \quad \mu_{\sigma,\lambda} = \Gamma_\Omega \mu_{\sigma,\lambda}^0, \quad (2.9)$$

with $(T_0, \mu_{\sigma,\lambda}^0)$ being the values of temperature and chemical potential on the rotation axis.

The above kinetic theory framework allows the classical contribution to the thermodynamic pressure of the system to be computed as

$$P_{\beta;\text{cl}} = \frac{1}{3} \sum_{\sigma,\lambda} \int dP E_{\mathbf{p}}^2 f_{\mathbf{p},\lambda}^{\text{eq};\sigma} = -\frac{T^4}{\pi^2} \sum_{\sigma,\lambda} \text{Li}_4(-e^{\mu_{\sigma,\lambda}/T}), \quad (2.10)$$

where $dP = d^3p/[(2\pi)^3 p^0]$ is the Lorentz-invariant momentum space integration measure, $E_{\mathbf{p}} = p \cdot u$ is the particle energy in the fluid rest frame and $\text{Li}_s(z) = \sum_{n=1}^{\infty} z^n/n^s$ is the polylogarithm. All other quantities can be computed from P_{cl} via thermodynamic derivatives, see Eq. (70) in Ref. [15]:

$$Q_{\ell;\beta;\text{cl}} = \frac{\partial P_{\beta;\text{cl}}}{\partial \mu_\ell}, \quad \sigma_{\ell;\beta;\text{cl}}^\omega = \frac{1}{2} \frac{\partial^2 P_{\beta;\text{cl}}}{\partial \mu_A \partial \mu_\ell}, \quad \sigma_{\ell;\beta;\text{cl}}^\tau = \frac{1}{12} \frac{\partial^3 P_{\beta;\text{cl}}}{\partial^2 \mu_A \partial \mu_\ell}, \quad (2.11)$$

while $\sigma_{\varepsilon;\text{cl}}^\omega = Q_{A;\text{cl}}$. Finally, $\pi_{1;\beta;\text{cl}} = -2\sigma_{A;\beta;\text{cl}}^\pi/27$ and $\pi_{2;\beta;\text{cl}} = -2\sigma_{A;\beta;\text{cl}}^\tau$ [see Eq. (94) in Ref. [15]], where $\sigma_{\ell;\beta;\text{cl}}^\pi = \frac{1}{2} \partial^4 P_{\text{cl}} / \partial^3 \mu_A \partial \mu_\ell$ [cf. Eq. (70) in Ref. [15]].

2.2 The Landau frame

In the case when the rotation is slow, one may neglect quadratic terms in Ω for a region close to the rotation axis. Since the vector τ^μ is of third order in Ω , it can be neglected, such that J_ℓ^μ and $T^{\mu\nu}$ simplify to

$$J_\ell^\mu \simeq Q_{\ell;\beta} u_\Omega^\mu + \sigma_{\ell;\beta}^\omega \omega_\Omega^\mu, \quad T^{\mu\nu} \simeq (E_\beta + P_\beta) u_\Omega^\mu u_\Omega^\nu - P_\beta g^{\mu\nu} + \sigma_{\varepsilon;\beta}^\omega (\omega_\Omega^\mu u_\Omega^\nu + u_\Omega^\mu \omega_\Omega^\nu), \quad (2.12)$$

where we used the subscript β to indicate that the above decomposition is performed with respect to the β -frame four-velocity, u_Ω^μ . Neglecting quadratic terms in Ω also implies that the quantum corrections to the above expressions can be ignored and, e.g., P_β can be safely replaced by $P_{\beta;\text{cl}}$ in Eq. (2.10). For notational convenience, we shall drop the ‘‘cl’’ subscript from all thermodynamic quantities in what follows.

We now seek to reexpress J_ℓ^μ and $T^{\mu\nu}$ with respect to the Landau frame. The latter frame is characterized by the four-velocity u_L^μ satisfying the eigenvalue equation $T^\mu{}_\nu u_L^\nu = E_L u_L^\mu$, where E_L represents the energy density of the fluid in the Landau frame. A particular feature of the Landau frame is that the heat-flux type of term is completely removed from $T^{\mu\nu}$, giving rise to the decomposition

$$J_\ell^\mu = Q_{\ell;L} u_L^\mu + V_{\ell;L}^\mu, \quad T^{\mu\nu} = (E_L + P_L) u_L^\mu u_L^\nu - P_L g^{\mu\nu} + \pi_L^{\mu\nu}. \quad (2.13)$$

Working under the assumption of small Ω , we can determine the Landau four-velocity up to first order with respect to Ω as

$$u_L^\mu = u_\Omega^\mu + \frac{\sigma_{\varepsilon;\beta}^\omega}{E + P} \omega_\Omega^\mu. \quad (2.14)$$

To linear order in Ω , the energy density, pressure and charge densities remain unchanged, $E_L = E_\beta \equiv E$, $P_L = P_\beta \equiv P$, and $Q_{L;\ell} = Q_{\beta;\ell} \equiv Q_\ell$, while the shear-stress tensor $\pi_L^{\mu\nu}$ is quadratic with respect to Ω and will, therefore, be disregarded. For notational convenience, we shall remove the L subscript for Landau-frame quantities. The vortical conductivities now absorb the vortical heat conductivity, as follows:

$$\sigma_\ell^\omega = \sigma_{\ell;\beta}^\omega - \frac{\sigma_{\varepsilon;\beta}^\omega Q_\ell}{E + P}. \quad (2.15)$$

Since we chose to ignore terms that are quadratic with respect to the angular frequency Ω , it is possible to employ one further simplification. We consider the Lorentz boost to the frame where the z component of the four-velocity vector u_L^μ vanishes:

$$L^{\mu\nu} = g^{\mu\nu} - \frac{\sigma_{\varepsilon;\beta}^\omega}{E + P} (u_\Omega^\mu \omega_\Omega^\nu + u_\Omega^\nu \omega_\Omega^\mu). \quad (2.16)$$

One can easily check that $u_L^\mu \rightarrow L^\mu{}_\nu u_L^\nu = u_\Omega^\mu + O(\Omega^2) \simeq u_\Omega^\mu$. To linear order, the vorticity vector ω_Ω^μ remains unchanged. Thus, in this boosted Landau frame, we have:

$$T^{\mu\nu} = (E + P)u^\mu u^\nu - P g^{\mu\nu}, \quad J_\ell^\mu = Q_\ell u^\mu + \sigma_\ell^\omega \omega^\mu, \quad (2.17)$$

where we dropped both the L and the Ω labels for notational brevity. All quantities appearing above are given by the classical expressions in Eqs. (2.10)–(2.11), i.e.

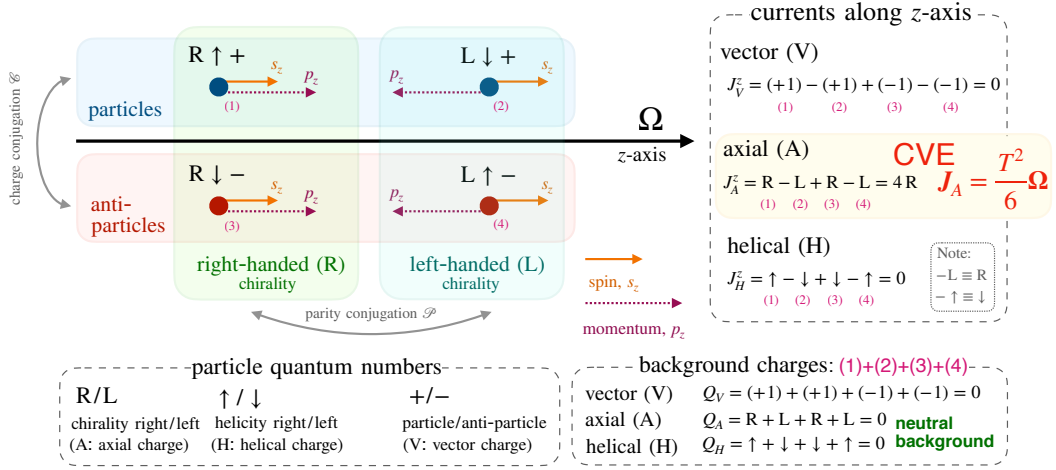
$$P = \frac{E}{3} \simeq -\frac{T^4}{\pi^2} \sum_{\sigma,\lambda} \text{Li}_4(-e^{\mu_{\sigma,\lambda}/T}), \quad Q_\ell \simeq \frac{\partial P}{\partial \mu_\ell}, \quad \sigma_\ell^\omega \simeq \frac{1}{2} \frac{\partial^2 P}{\partial \mu_\ell \partial \mu_A} - \frac{Q_\ell Q_A}{E + P}. \quad (2.18)$$

2.3 Vector/axial/helical anomalous vortical transport as spin-orbit coupling

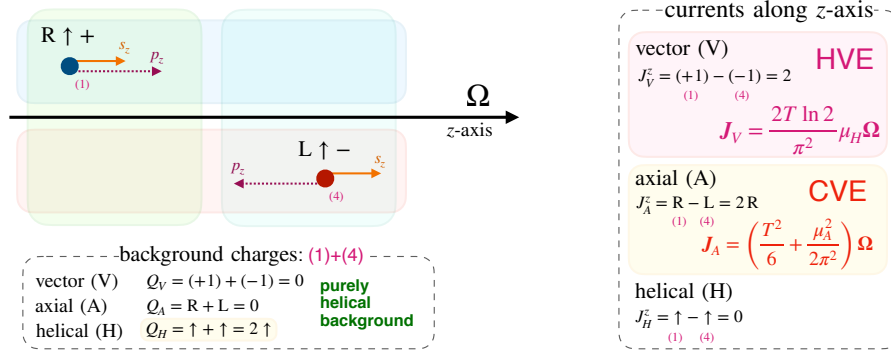
Before addressing the technical details of explicit calculations of the hydrodynamic wave spectrum, it is necessary to discuss certain simple and easily understandable examples of anomalous vortical transport. Our calculations involve the helical degree of freedom, which is often misidentified with the chiral property of a fermion. As we highlighted in the Introduction, the chirality and helicity – that are related, for a single (anti-)fermion, to each other via Eq. (1.1) – are distinct quantities of fermionic ensembles that constitute different properties of a many-body fermionic system. This distinction also reveals itself at the level of anomalous transport.

It is worth noticing that the vortical conductivities defined in the Landau frame (2.15) and in the β frame differ from each other due to the freedom of interpreting the heat flux as particle diffusion and vice-versa, see Eq. (2.15). However, in the physically interesting high-temperature limit, the leading contributions to the anomalous conductivities in the β frame and in the Landau frame – which will be given below in Eqs. (3.5e) and (3.5f), respectively – are the same for both frames up to subleading $O(T^0)$ corrections and they agree qualitatively, up to a numerical factor, even in the $O(T^{-1})$ order. Explicitly, the leading anomalous vector, axial and helical conductivities in the β frame read, respectively,

(a) Chiral Vortical Effect: Axial current in neutral background ($\mu_V = 0$, $\mu_A = 0$, $\mu_H = 0$, $T \neq 0$)



(b) Helical Vortical Effect: Vector current in helical background ($\mu_V = 0$, $\mu_A = 0$, $\mu_H \neq 0$, $T \neq 0$)



(c) Helical Vortical Effect: Helical current in vector background ($\mu_V \neq 0$, $\mu_A = 0$, $\mu_H = 0$, $T \neq 0$)

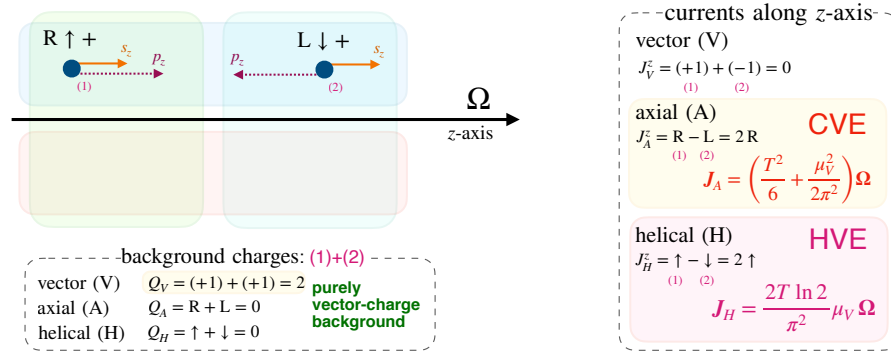


Figure 1: Generation of chiral and helical vortical effects due to spin-orbit coupling in fermion–anti-fermion ensembles rotating with the angular velocity Ω . An elementary counting of vector, axial, and helical degrees of freedom explains the emergence of (a) the Chiral Vortical Effect (2.19a) in a neutral plasma as well as the Helical Vortical Effects (2.19b) and (2.19c) in the helically imbalanced (b) and degenerate (c) plasma. The chirality of particles is denoted by the letters R/L; their helicity is shown by the arrows \uparrow / \downarrow ; the vector charge is presented by the signs $+/-$. The counting gives the total charges, Q_ℓ and the z -axis projection of the currents J_ℓ^z , with $\ell = V, A, H$ for each case.

as follows [45]:

$$\sigma_{\beta;A}^{\omega} = \frac{T^2}{6} + \frac{1}{2\pi^2}(\mu_V^2 + \mu_A^2 + \mu_H^2) + O(T^{-1}), \quad (2.19a)$$

$$\sigma_{\beta;V}^{\omega} = \frac{2T \ln 2}{\pi^2} \mu_H + \frac{\mu_V \mu_A}{\pi^2} + O(T^{-1}), \quad (2.19b)$$

$$\sigma_{\beta;H}^{\omega} = \frac{2T \ln 2}{\pi^2} \mu_V + \frac{\mu_H \mu_A}{\pi^2} + O(T^{-1}). \quad (2.19c)$$

In the first term of Eq. (2.19a), we immediately recognize the Chiral Vortical Effect [11, 12], which appears as a result of the axial-gravitational anomaly [46]. Despite its anomalous origin, the emergence of the Chiral Vortical Effect (2.19a) can be readily understood on the basis of a simple particle counting of spin degrees of freedom in the system of the chiral fermions polarized in the presence of the vortical (rotating) background. Below, we also demonstrate that the Helical Vortical Effects, given in Eqs. (2.19b) and (2.19c), appear naturally on the very same basis as its famous chiral partner (2.19a). To this end, we give in Fig. 1 a pictorial counting for all three effects in Eqs. (2.19) to demonstrate its common origin.

All illustrations in Fig. 1 are based on the simple fact that the chiralities and helicities are equal (opposite) for particles (antiparticles). The charge conjugation \mathcal{C} transforms a particle to its antiparticle ($q \rightarrow -q$) and, at the same time, flips its helicity ($\uparrow / \downarrow \rightarrow \downarrow / \uparrow$) while leaving intact its chirality ($R/L \rightarrow R/L$). These properties are consistent with the observation that helicity, similarly to the vector charge of the particle, is a \mathcal{P} -odd quantity while the chirality is a \mathcal{P} -even characteristic of the fermion. On the other hand, the parity transformation \mathcal{P} does not, expectedly, affect the vector charge, while it naturally flips both helicity ($\uparrow / \downarrow \rightarrow \downarrow / \uparrow$) and chirality ($R/L \rightarrow R/L$), which are \mathcal{P} -odd quantities. These properties are consistent with Eq. (1.1) and are summarized in Table 1 below. As seen in Table 1, the \mathcal{C} parities of the spatial currents \mathbf{J}_V , \mathbf{J}_A and \mathbf{J}_H are identical with those of the corresponding charges, while their \mathcal{P} and \mathcal{T} parities are reversed. The \mathcal{P} and \mathcal{T} parities of the currents \mathbf{J}_ℓ are identically shared by the product $Q_\ell p^z$, where p^z is the z -axis momentum of a hypothetical plasma constituent. Therefore, a simple, qualitative explanation of the macroscopic, ensemble-averaged, vortical effects can be visualized pictographically by considering individual constituents and their direction of motion, as indicated in Fig. 1.

The natural appearance of the Chiral Vortical Effect (2.19a) in a system of rotating chiral fermions is illustrated in Fig. 1(a). The spin-orbital interaction couples the orbital motion of the fermion-anti-fermion ensemble with the polarization of the spin of each particle. The particle spin \mathbf{s} tends to align with the angular velocity $\boldsymbol{\Omega}$ regardless of the charge of the particle, as the spin-orbital coupling does not discriminate between particles and antiparticles. In Fig. 1(a), we show, for simplicity, a maximally spin-polarized ensemble with the spins of all constituents \mathbf{s} aligned along the angular velocity $\boldsymbol{\Omega}$. The ensemble is neutral in all possible charges as the total vector, axial and helical numbers are zero. To achieve total neutrality of a non-empty ensemble, one needs at least four constituents: one (chirally) right-handed particle and a left-handed particle as well as their antiparticles, as

	Q_V	Q_A	Q_H	\mathbf{J}_V	\mathbf{J}_A	\mathbf{J}_H	\mathbf{v}	$\boldsymbol{\Omega}$
\mathcal{C}	-	+	-	-	+	-	+	+
\mathcal{P}	+	-	-	-	+	+	-	+
\mathcal{T}	+	+	+	-	-	-	-	-

Table 1: The charge conjugation \mathcal{C} , the parity inversion \mathcal{P} , and the time reversal \mathcal{T} symmetries of the vector Q_V , axial Q_A , and helical Q_H charges their currents, \mathbf{J}_ℓ ($\ell = V, A, H$), as well as the group velocity $\mathbf{v} = \partial\omega/\partial\mathbf{k}$ and the vorticity $\boldsymbol{\Omega}$. The signs $+/-$ indicate the even/odd nature of these quantities under the corresponding inversions.

it is shown in the figure. A simple counting, reproduced in this figure as well, shows that the spin polarization in this ensemble generates an axial current along the axis of rotation, $\mathbf{j}_A \propto \boldsymbol{\Omega}$, while the vector and helical currents vanish identically. This simple picture based on degree-counting is perfectly consistent with the prediction of the anomalous transport laws (2.19) for the neutral plasma (with $\mu_V = \mu_A = \mu_H = 0$).

An immediate emergence of one of the Helical Vortical Effects (2.19b) is illustrated in Fig. 1(b). Here, we consider a helically nontrivial background where the helical charge is non-zero while all other (vector and axial) charges are vanishing. To achieve this set of quantum numbers, it is sufficient to take a chirally right-handed particle and a chirally left-handed antiparticle. One quickly arrives at the conclusion that in this ensemble, the spin polarization produces the vector current along the angular velocity: $\mathbf{J}_V \propto \boldsymbol{\Omega}$. The axial current is also generated in consistency with Eq. (2.19a).

Figure 1(c) shows that in the presence of a vector charge (one right-handed particle and one left-handed particle), the spin-orbit coupling generates the helical current $\mathbf{J}_H \propto \boldsymbol{\Omega}$ along the axis of rotation as follows from the other type of the Helical Vortical Effect (2.19c). The axial current is again generated in consistency with Eq. (2.19a).

Finally, to close our considerations, we consider the purely axial background. Then the anomalous vortical effects (2.19) predict that such an ensemble may only lead to an axial current (2.19a), while the vector (2.19b) and helical (2.19c) currents should vanish. It is not difficult to check these properties following our considerations in Fig. 1, by considering, for example, an ensemble made of one chirally right-handed particle and its antiparticle.

Thus, the chirality and helicity are independent numbers that appear naturally in the fermionic systems containing both particles and antiparticles. As we have just seen, the presence of helical charge generates the vector current while the excess of vector charge produces the helical flow along the axis of rotation. Both the helical and vector charge densities produce the axial current. These anomalous transport effects, presented in Eq. (2.19) and qualitatively justified by the counting of Fig. 1, intertwine the vector, axial and helical degrees of freedom in the form of hydrodynamic excitations. The rigorous investigation of these hydrodynamic effects is the subject of the present paper.

2.4 Conservation equations for longitudinal perturbations

We now consider small perturbations around the rigidly rotating state in terms of fluctuations of velocity, charge densities, and pressure. While doing so, we assume that the constitutive Eqs. (2.17) continue to hold, with the quantities E , Q_ℓ and σ_ℓ^ω derived from P as in Eq. (2.18), u^μ being now the perturbed velocity and ω^μ the perturbed vorticity associated to u^μ . Perturbations in the chemical potentials μ_ℓ and temperature T are subsequently induced by the relations

$$\delta P = \frac{\partial P}{\partial T} \delta T + \frac{\partial P}{\partial \mu_\ell} \delta \mu_\ell, \quad \delta Q_\ell = \frac{\partial Q_\ell}{\partial T} \delta T + \frac{\partial Q_\ell}{\partial \mu_{\ell'}} \delta \mu_{\ell'}, \quad (2.20)$$

with $\partial P / \partial T = s = (E + P - \vec{Q} \cdot \vec{\mu}) / T$ being the entropy density and $\partial P / \partial \mu_\ell = Q_\ell$. We consider the limit of slow rotation and continue to retain only terms that are linear in the angular frequency Ω . For consistency, we focus on the region around the rotation axis, where $\rho \Omega \ll 1$.

In this paper, we are interested in the study of the propagation of perturbations along the axis of rotation (the z axis). Decomposing the time-dependent four-velocity $\bar{u}^\mu \equiv \bar{u}^\mu(t, z)$, charge densities $\bar{Q}_\ell \equiv \bar{Q}_\ell(t, z)$ and pressure $\bar{P} \equiv \bar{P}(t, z)$ into a background contribution (denoted without the overline) and a perturbation,

$$\bar{u}^\mu = u^\mu \partial_\mu + \delta \bar{u}^\mu, \quad \bar{Q}_\ell = Q_\ell + \delta \bar{Q}_\ell, \quad \bar{P} = P + \delta \bar{P}, \quad (2.21)$$

we expand the perturbations $\delta \bar{u}^\mu$, $\delta \bar{Q}_\ell$ and $\delta \bar{P}$ in a Fourier series,

$$\begin{pmatrix} \delta \bar{u}^\mu \\ \delta \bar{Q}_\ell \\ \delta \bar{P}_\ell \end{pmatrix} = \int_{-\infty}^{\infty} dk e^{ikz} \sum_{\omega} e^{-i\omega t} \begin{pmatrix} \delta u_\omega^\mu(k) \\ \delta Q_{\ell;\omega}(k) \\ \delta P_\omega(k) \end{pmatrix}, \quad (2.22)$$

where $\omega \equiv \omega(k)$ is the angular frequency, which is related to the wavenumber k via the dispersion relation. Note that the vorticity four-vector, ω^μ , always carries a Lorentz four-index, whereas its magnitude is denoted by Ω , such that there is no risk of confusion with the angular frequency ω . The background four-velocity $u^\mu \equiv u_\Omega^\mu$ is introduced in Eq. (2.2) and corresponds to that of a rigidly-rotating fluid, while the background pressure and charge densities are assumed to be constant. Notice that the perturbation mode amplitudes for the four-velocity, δu_ω , charge densities, $\delta Q_{\ell;\omega}$, and pressure, δP_ω , can take complex values corresponding to a (relative) phase of these fluctuations.

For simplicity, in this work, we focus only on longitudinal perturbations of the velocity, such that $\delta u_\omega^\mu \partial_\mu = \delta u_\omega \partial_z$. These perturbations in the velocity induce a perturbation in the vorticity,

$$\bar{\omega}^\mu \partial_\mu = \Omega \partial_z + \Omega \int_{-\infty}^{\infty} dk e^{ikz} \sum_{\omega} e^{-i\omega t} \delta u_\omega \left(\partial_t - \frac{i}{2} \omega \rho \partial_\rho \right). \quad (2.23)$$

The projector $\bar{\Delta}^{\mu\nu} = \Delta^{\mu\nu} + \delta\Delta^{\mu\nu}$ is given by its background value corresponding to rigid rotation [cf. also Eq. (2.5)], and the perturbation $\delta\bar{\Delta}^{\mu\nu} = \int_{-\infty}^{\infty} e^{ikz} \sum_{\omega} e^{-i\omega t} \delta\Delta_{\omega}^{\mu\nu}$, satisfying

$$\Delta^{\mu\nu} = \begin{pmatrix} 0 & y\Omega & -x\Omega & 0 \\ y\Omega & -1 & 0 & 0 \\ -x\Omega & 0 & -1 & 0 \\ 0 & 0 & 0 & -1 \end{pmatrix}, \quad \delta\Delta_{\omega}^{\mu\nu} = \delta u_{\omega} \begin{pmatrix} 0 & 0 & 0 & -1 \\ 0 & 0 & 0 & y\Omega \\ 0 & 0 & 0 & -x\Omega \\ -1 & y\Omega & -x\Omega & 0 \end{pmatrix}. \quad (2.24)$$

We are now ready to set up the linear perturbations problem. For this purpose, we assume, as stated in the introduction of this section, that the stress-energy tensor $T^{\mu\nu}$ and the charge currents J_{ℓ}^{μ} are given as in Eqs. (2.17). The dynamics of the velocity and pressure perturbations follow by imposing the conservation of energy and momentum, $\partial_{\mu}T^{\mu\nu} = 0$, leading to

$$DE + (E + P)\theta = 0, \quad (E + P)Du^{\mu} - \nabla^{\mu}P = 0, \quad (2.25a)$$

where $D = u^{\mu}\partial_{\mu}$ represents the comoving derivative, $\nabla^{\mu} = \Delta^{\mu\nu}\partial_{\nu}$ is the spatial gradient in the fluid rest frame, while $\theta = \partial_{\mu}u^{\mu}$ is the expansion scalar. For simplicity, the overhead bars were dropped in the above equations, however we understand that they will hold also for the perturbed quantities.

Furthermore, we impose the conservation of the charge currents, $\partial_{\mu}J_{\ell}^{\mu} = 0$, with $\ell \in \{V, A, H\}$. All three currents are conserved in the quantum field theory of free (non-interacting) massless fermions. This is certainly true also in the quantum case for the vector current. In a realistic interacting theory, the conservation of the axial current is broken by the axial anomaly [47–49]. Moreover, interactions mediated by vector bosons (photons in QED or gluons in QCD) break the helicity current conservation through the so-called helicity-violating pair annihilation (HVPA) processes (cf. Sec. 5.2 in Ref. [25]). We address such effects in detail in our companion paper [26] and instead consider in this paper that all three charge currents are conserved. Then, $\partial_{\mu}J_{\ell}^{\mu} = 0$ leads to:

$$DQ_{\ell} + Q_{\ell}\theta + \omega^{\mu}\partial_{\mu}\sigma_{\ell}^{\omega} + \sigma_{\ell}^{\omega}\partial_{\mu}\omega^{\mu} = 0. \quad (2.25b)$$

The terms appearing in Eqs. (2.25) above can be computed by going to Fourier space, which amounts to the following substitutions:

$$\begin{aligned} Df &\rightarrow -i\omega\delta f_{\omega}, & \theta &\rightarrow ik\delta u_{\omega}, & \partial_{\mu}\omega^{\mu} &\rightarrow -2i\omega\Omega\delta u_{\omega}, \\ \omega^{\mu}\partial_{\mu}\sigma_{\ell}^{\omega} &\rightarrow ik\Omega \left(\frac{\partial\sigma_{\ell}^{\omega}}{\partial P}\delta P_{\omega} + \sum_{\ell'=V,A,H} \frac{\partial\sigma_{\ell}^{\omega}}{\partial Q_{\ell'}}\delta Q_{\ell';\omega} \right), \\ Du^{\mu} &\rightarrow -i\omega\delta_z^{\mu}\delta u_{\omega}, & \nabla^{\mu}P &\rightarrow -i[\omega\Omega(y\delta_x^{\mu} - x\delta_y^{\mu}) + k\delta_z^{\mu}]\delta P_{\omega}, \end{aligned} \quad (2.26)$$

where f is a scalar function and the right arrow indicates projecting the quantities to the left onto the $(k, \omega(k))$ Fourier mode.

It is clear that the stress-energy sector is decoupled from the charge currents sector since it involves only the amplitudes δu_{ω} and δP_{ω} , which satisfy the following closed set of

equations:

$$\begin{pmatrix} -3\omega & 4kP \\ k & -4P\omega \end{pmatrix} \begin{pmatrix} \delta P_\omega \\ \delta u_\omega \end{pmatrix} = 0, \quad (2.27)$$

There are two independent solutions to the above equation, which are obtained by the requirement that the determinant of the matrix on the left-hand side of Eq. (2.27) vanishes:

$$3\omega^2 - k^2 = 0. \quad (2.28)$$

This relation gives rise to the acoustic modes,

$$\omega_{\text{ac.}}^\pm = \pm c_s k, \quad c_s = 1/\sqrt{3}, \quad (2.29)$$

with c_s being the speed of sound in an ultrarelativistic ideal fluid. To leading order in Ω , Eq. (2.27) admits also $\delta u_\omega = \delta P_\omega = 0$ as a trivial solution.

The charge conservation condition in Eq. (2.25) gives us the following set of equations:

$$\sum_{\ell'=V,A,H} \left(\omega \delta_{\ell,\ell'} - k\Omega \frac{\partial \sigma_\ell^\omega}{\partial Q_{\ell'}} \right) \delta Q_{\ell';\omega} - k\Omega \frac{\partial \sigma_\ell^\omega}{\partial P} \delta P_\omega - (kQ_\ell - 2\omega\Omega \sigma_\ell^\omega) \delta u_\omega = 0, \quad (2.30)$$

where we have adopted a unified notation to refer to all three charges, $\ell \in \{V, A, H\}$.

Below, we focus on the hydrodynamic modes characterized by fluctuations of charge densities and their currents, thus neglecting the purely acoustic modes. Setting $\delta u_\omega = \delta P_\omega = 0$ in Eq. (2.30) leads to

$$\left(\omega \delta Q_{\ell;\omega} - k\Omega \delta \sigma_{\ell;\omega}^\omega \right) \Big|_{\delta P_\omega=0} = 0. \quad (2.31)$$

The above equation, written with respect to the fluctuations $\delta Q_{\ell;\omega}$ of the charge densities, can be reexpressed in terms of fluctuations in the chemical potentials, $\delta \mu_{\ell;\omega}$, as well as fluctuations in temperature, δT_ω . Due to the constraint $\delta P_\omega = 0$, these fluctuations are not mutually independent. In fact, taking into account that $\delta P_\omega = s\delta T_\omega + \sum_\ell Q_\ell \delta \mu_{\ell;\omega}$, one may replace δT_ω via

$$\delta T_\omega = - \sum_\ell \frac{Q_\ell}{s} \delta \mu_{\ell;\omega}. \quad (2.32)$$

Subsequently, this replacement leads to the following system of equations for the perturbations in the chemical potentials:

$$\sum_{\ell'} \mathbb{M}_{\ell\ell'} \delta \mu_{\ell';\omega} = 0, \quad \mathbb{M}_{\ell\ell'} \equiv \mathbb{M}_{\ell\ell'}(k, \omega) = \frac{\omega}{s} \frac{\partial(P, Q_\ell)}{\partial(T, \mu_{\ell'})} - \frac{k\Omega}{s} \frac{\partial(P, \sigma_\ell^\omega)}{\partial(T, \mu_{\ell'})}, \quad (2.33)$$

where it is understood that all quantities appearing in the expression for $\mathbb{M}_{\ell,\ell'}$ are evaluated in the background state of the fluid. In the above, we employed the standard notation for the Jacobian,

$$\frac{\partial(f, g)}{\partial(x, y)} = \frac{\partial f}{\partial x} \frac{\partial g}{\partial y} - \frac{\partial f}{\partial y} \frac{\partial g}{\partial x}. \quad (2.34)$$

Nontrivial solutions for ω can be obtained by requiring that the determinant of the matrix \mathbb{M} vanishes. Noting that $Q_\ell = \partial P / \partial \mu_\ell$, we can rewrite its temperature derivative as follows:

$$\frac{\partial Q_\ell}{\partial T} = \frac{\partial s}{\partial \mu_\ell} = \frac{3Q_\ell}{T} - \frac{\vec{\mu}}{T} \cdot \frac{\partial Q_\ell}{\partial \vec{\mu}}, \quad (2.35)$$

where we took into account that $s = (E + P - \vec{\mu} \cdot \vec{Q})/T$, as well as the relation $\partial \vec{Q} / \partial \mu_\ell = \partial Q_\ell / \partial \vec{\mu}$. Similarly, taking into account that $\sigma_{\ell;\beta}^\omega = \frac{1}{2} \partial Q_\ell / \partial \mu_A$ and $\sigma_\ell^\omega = \sigma_{\ell;\beta}^\omega - Q_A Q_\ell / (E + P)$, we have

$$\frac{\partial \sigma_{\ell;\beta}^\omega}{\partial T} = \frac{2\sigma_{\ell;\beta}^\omega}{T} - \frac{\vec{\mu}}{T} \frac{\partial \sigma_{\ell;\beta}^\omega}{\partial \vec{\mu}}, \quad \frac{\partial \sigma_\ell^\omega}{\partial T} = \frac{2\sigma_\ell^\omega}{T} - \frac{\vec{\mu}}{T} \frac{\partial \sigma_\ell^\omega}{\partial \vec{\mu}}. \quad (2.36)$$

Therefore, the matrix elements $\mathbb{M}_{\ell,\ell'}$ can be expressed as

$$\begin{aligned} \mathbb{M}_{\ell\ell'} &= \omega \left(\frac{\partial Q_\ell}{\partial \mu_{\ell'}} - \frac{Q_{\ell'}}{s} \frac{\partial Q_\ell}{\partial T} \right) - k\Omega \left(\frac{\partial \sigma_\ell^\omega}{\partial \mu_{\ell'}} - \frac{Q_{\ell'}}{s} \frac{\partial \sigma_\ell^\omega}{\partial T} \right) \\ &= \omega T^2 \mathbb{M}_{\ell\ell'}^\omega - k\Omega T \mathbb{M}_{\ell\ell'}^\Omega, \end{aligned} \quad (2.37a)$$

where we introduced for later convenience the following notation:

$$\mathbb{M}_{\ell\ell'}^\omega = \frac{1}{T^2} \left(\frac{\partial Q_\ell}{\partial \mu_{\ell'}} - \frac{3Q_\ell Q_{\ell'}}{sT} + \frac{Q_{\ell'} \vec{\mu}}{sT} \cdot \frac{\partial Q_\ell}{\partial \vec{\mu}} \right), \quad (2.37b)$$

$$\mathbb{M}_{\ell\ell'}^\Omega = \frac{1}{T} \left(\frac{\partial \sigma_\ell^\omega}{\partial \mu_{\ell'}} - \frac{2\sigma_\ell^\omega Q_{\ell'}}{sT} + \frac{Q_{\ell'} \vec{\mu}}{sT} \cdot \frac{\partial \sigma_\ell^\omega}{\partial \vec{\mu}} \right). \quad (2.37c)$$

The structure of the matrix $\mathbb{M}_{\ell\ell'}$ shows that the angular velocities $\omega(k)$ obey linear dispersion relations,

$$\omega = kv, \quad (2.38)$$

where $v = \omega/k = \partial \omega / \partial k$ represents both the phase and the group velocity of the given excitation mode, being independent on wavenumber k .

2.5 Full space-time solutions from Fourier modes

Let us consider a function $\bar{f}(t, z)$ characterizing the fluid state, taking the value f in the background fluid state. Under small perturbations, $\delta \bar{f}(t, z) = \bar{f}(t, z) - f$ can be expanded with respect to the Fourier modes considered in Eq. (2.22) as follows:

$$\delta \bar{f}(t, z) = \int_{-\infty}^{\infty} dk e^{ikz} \sum_{\omega} e^{-i\omega(k)t} \delta f[k, \omega(k)], \quad (2.39)$$

where $\delta f[k, \omega(k)]$ represent the Fourier mode amplitudes. In the above, we have anticipated that the system supports only a discrete number of angular frequencies, characterized by the dispersion relation $\omega \equiv \omega(k)$. Let us look at the complex conjugate of $\bar{f}(t, z)$:

$$\bar{f}^*(t, z) = f^* + \int_{-\infty}^{\infty} dk e^{ikz} \sum_{\omega} e^{i\omega^*(-k)t} \delta f^*[-k, \omega(-k)] \quad (2.40)$$

Imposing that $\bar{f}(t, z)$ is real implies that

$$\omega^*(-k) = -\omega(k), \quad \delta f^*[-k, \omega(-k)] = \delta f[k, \omega(k)], \quad (2.41)$$

while $f^* = f$. This imposes the structure

$$\omega(k) = kC_\omega(k) - iD_\omega(k), \quad (2.42)$$

where the phase velocity $C_\omega(k) = \text{Re}[\omega(k)/k]$ and the dissipation rate $D_\omega(k) = -\text{Im}[\omega(k)]$ are both real and even with respect to $k \rightarrow -k$. The modes allowed by the matrix $\mathbb{M}_{\ell\ell'}$ have the linear dispersion relation $\omega = vk$, hence $C_\omega(k) = v$ and $D_\omega(k) = 0$. Using the above notation, Eq. (2.39) can be written as

$$\delta\bar{f}(t, z) = 2 \int_0^\infty dk \sum_\omega \{ \cos(kvt - kz) \text{Re}[\delta f(k, \omega(k))] - \sin(kvt - kz) \text{Im}[\delta f(k, \omega(k))] \}. \quad (2.43)$$

Frequently, we will consider the case when one of the chemical potentials (the representative one) is initialized according to a simple, harmonic cosine profile, achieved by setting

$$\bar{f}(0, z) = f + \delta\bar{f}_0 \cos(kz). \quad (2.44)$$

This implies that the mode amplitudes $\delta f(k', \omega(k'))$ satisfy

$$\delta f(k', \omega(k')) = \frac{1}{2} \delta f_\omega [\delta(k' - k) + \delta(k' + k)], \quad (2.45)$$

which is compatible with Eq. (2.41). The constants δf_ω must satisfy

$$\sum_\omega \delta f_\omega = \delta\bar{f}_0, \quad (2.46)$$

and the space-time solution reads

$$\delta\bar{f}(t, z) = \sum_\omega \delta f_\omega \cos(kz - kvt), \quad (2.47)$$

with $v = \omega/k$ being independent of k .

Finally, we will consider the case of an initial Gaussian profile,

$$\bar{f}(0, z) = f + \delta\bar{f}_0 e^{-z^2/2\sigma^2}. \quad (2.48)$$

The mode amplitudes then satisfy

$$\sum_\omega \delta f(k, \omega(k)) = \frac{\sigma}{\sqrt{2\pi}} \delta\bar{f}_0 e^{-\sigma^2 k^2/2}. \quad (2.49)$$

The exact expression for each mode amplitude $\delta f_k \equiv \delta f(k, \omega(k))$ depends on the conditions imposed at the level of the three independent chemical potentials, $\delta\bar{\mu}_{\ell;0} \equiv \delta\bar{\mu}_\ell(0, z)$. Retrieving the space-time solution $\delta\bar{f}(t, z)$ requires the inverse Gaussian integration formula,

$$\frac{\sigma}{\sqrt{2\pi}} \int_{-\infty}^\infty e^{-i\omega t + ikz} e^{-\sigma^2 k^2/2} dk = e^{-(z-vt)^2/2\sigma^2}, \quad (2.50)$$

where we used the property that $\omega = kv$ and v is independent of k .

3 Hydrodynamic waves at high temperature

In the large temperature limit, we may assume that $|\mu_\ell| \ll T$, allowing the polylogarithms in Eq. (2.10) to be expanded in a Taylor series with respect to the dimensionless chemical potentials $\alpha_\ell = \mu_\ell/T$. Using the definition of the polylogarithm,

$$\text{Li}_4(-e^{\mu_{\sigma,\lambda}/T}) = \sum_{n=1}^{\infty} \frac{(-1)^n}{n^4} e^{n\mu_{\sigma,\lambda}/T}, \quad (3.1)$$

we can expand the exponential in a Taylor series. The sum over n can be performed employing the identity $\sum_{n=1}^{\infty} (-1)^n/n^s = -(1-2^{1-s})\zeta(s)$, where $\zeta(s)$ is the Riemann zeta function. This procedure leads us to a number of useful identities:

$$\begin{aligned} \sum_{n=1}^{\infty} \frac{(-1)^n}{n^4} &= -\frac{7\pi^4}{720}, & \sum_{n=1}^{\infty} \frac{(-1)^n}{n^3} &= -\frac{3\zeta(3)}{4}, & \sum_{n=1}^{\infty} \frac{(-1)^n}{n^2} &= -\frac{\pi^2}{12}, \\ \sum_{n=1}^{\infty} \frac{(-1)^n}{n} &= -\ln 2, & \sum_{n=1}^{\infty} (-1)^n &\rightarrow -\frac{1}{2}, \end{aligned} \quad (3.2)$$

where the last relation follows only under the assumption of analytical continuation of the ζ function. The summation over the numbers $\sigma = \pm 1$ and $\lambda = \pm 1/2$ can be performed using the relations:

$$\begin{aligned} \sum_{\sigma,\lambda} 1 &= 4, & \sum_{\sigma,\lambda} \mu_{\sigma,\lambda} &= 0, & \sum_{\sigma,\lambda} \mu_{\sigma,\lambda}^2 &= 4\bar{\mu}^2, & \sum_{\sigma,\lambda} \mu_{\sigma,\lambda}^3 &= 24\mu_\times^3, \\ \sum_{\sigma,\lambda} \mu_{\sigma,\lambda}^4 &= 4(\bar{\mu}^2)^2 + 16(\mu_V^2\mu_H^2 + \mu_V^2\mu_A^2 + \mu_A^2\mu_H^2), \end{aligned} \quad (3.3)$$

where we employed Eq. (1.1) to perform the sums and introduced the following notation:

$$\bar{\mu}^2 = \mu_V^2 + \mu_A^2 + \mu_H^2, \quad \mu_\times^3 = \mu_V\mu_A\mu_H. \quad (3.4)$$

We therefore obtain for the pressure:

$$P = \frac{7\pi^2 T^4}{180} + \frac{\bar{\mu}^2 T^2}{6} + \frac{4\mu_\times^3 T}{\pi^2} \ln 2 + \frac{(\bar{\mu}^2)^2}{12\pi^2} + \frac{\mu_A^2\mu_H^2 + \mu_V^2\mu_H^2 + \mu_V^2\mu_A^2}{3\pi^2} + O(T^{-1}), \quad (3.5a)$$

The charge densities Q_ℓ and entropy density s can be found via the following thermodynamic relations (2.11):

$$Q_\ell = \frac{\mu_\ell T^2}{3} + \frac{4T \ln 2}{\pi^2} \frac{\partial \mu_\times^3}{\partial \mu_\ell} + \frac{\mu_\ell (3\bar{\mu}^2 - 2\mu_\ell^2)}{3\pi^2} + O(T^{-1}), \quad (3.5b)$$

$$s = \frac{7\pi^2 T^3}{45} + \frac{\bar{\mu}^2 T}{3} + \frac{4\mu_\times^3}{\pi^2} \ln 2 + O(T^{-2}), \quad (3.5c)$$

where it is understood that no summation over ℓ is implied in the last term in the above expression for Q_ℓ . In order to find the terms appearing in the matrix $\mathbb{M}_{\ell\ell'}$ given in Eq. (2.37),

the derivative of the charge densities with respect to the chemical potential must be computed:

$$\frac{\partial Q_\ell}{\partial \mu_{\ell'}} = \frac{\delta_{\ell\ell'} T^2}{3} + \frac{4T \ln 2}{\pi^2} \frac{\partial^2 \mu_\times^3}{\partial \mu_\ell \partial \mu_{\ell'}} + \frac{\delta_{\ell\ell'} (\bar{\mu}^2 - 2\mu_\ell^2) + 2\mu_\ell \mu_{\ell'}}{\pi^2} + O(T^{-1}), \quad (3.5d)$$

where again, there is no summation with respect to ℓ in the last term appearing above. The β -frame vortical conductivities can be obtained from Eq. (2.11) as:

$$\sigma_{\beta;\ell}^\omega = \frac{\delta_{\ell A} T^2}{6} + \frac{2T \ln 2}{\pi^2} (\mu_V \delta_{\ell H} + \mu_H \delta_{\ell V}) + \frac{\delta_{\ell A}}{2\pi^2} (\mu_V^2 - \mu_A^2 + \mu_H^2) + \frac{\mu_\ell \mu_A}{\pi^2} + O(T^{-1}). \quad (3.5e)$$

Noting that $Q_\ell Q_{\ell'} / (E + P) = 5\mu_\ell \mu_{\ell'} / 7\pi^2 + O(T^{-1})$, the Landau frame vortical conductivities introduced in Eq. (2.15) can be seen to differ from $\sigma_{\beta;\ell}^\omega$ only in the $O(T^0)$ term:

$$\sigma_\ell^\omega = \frac{\delta_{\ell A} T^2}{6} + \frac{2T \ln 2}{\pi^2} (\mu_V \delta_{\ell H} + \mu_H \delta_{\ell V}) + \frac{\delta_{\ell A}}{2\pi^2} (\mu_V^2 - \mu_A^2 + \mu_H^2) + \frac{2\mu_\ell \mu_A}{7\pi^2} + O(T^{-1}). \quad (3.5f)$$

Their derivatives with respect to the chemical potentials are

$$\frac{\partial \sigma_\ell^\omega}{\partial \mu_{\ell'}} = \frac{2T \ln 2}{\pi^2} (\delta_{\ell V} \delta_{\ell' H} + \delta_{\ell H} \delta_{\ell' V}) + \frac{\delta_{\ell A}}{\pi^2} (\mu_{\ell'} - 2\mu_A \delta_{\ell' A}) + \frac{2}{7\pi^2} (\delta_{\ell\ell'} \mu_A + \mu_\ell \delta_{\ell' A}) + O(T^{-1}). \quad (3.5g)$$

With the above results, the matrices \mathbb{M}_ω and \mathbb{M}_Ω defined in Eq. (2.37) can be expanded as follows:

$$\begin{aligned} \mathbb{M}_\omega &= \frac{1}{3} \mathbb{I} + \frac{4 \ln 2}{\pi^2 T} \begin{pmatrix} 0 & \mu_H & \mu_A \\ \mu_H & 0 & \mu_V \\ \mu_A & \mu_V & 0 \end{pmatrix} + O(T^{-2}), \\ \mathbb{M}_\Omega &= \frac{2 \ln 2}{\pi^2} \begin{pmatrix} 0 & 0 & 1 \\ 0 & 0 & 0 \\ 1 & 0 & 0 \end{pmatrix} + \frac{2}{7\pi^2 T} \begin{pmatrix} \mu_A & \mu_V & 0 \\ \mu_V & -4\mu_A & \mu_H \\ 0 & \mu_H & \mu_A \end{pmatrix} + O(T^{-2}), \end{aligned} \quad (3.6)$$

where \mathbb{I} is the unit matrix.

The equation $\det(\mathbb{M}/T^2) = 0$ can be solved iteratively, using the formula

$$\det(\mathbb{A} + \varepsilon \mathbb{B}) = \det(\mathbb{A}) [1 + \varepsilon \text{tr}(\mathbb{A}^{-1} \mathbb{B}) + O(\varepsilon^2)], \quad (3.7)$$

which is valid for small ε . Considering now a large- T expansion of the angular frequency ω ,

$$\omega = \omega_0 + \frac{\omega_1}{T} + \frac{\omega_2}{T^2} + O(T^{-3}), \quad (3.8)$$

it is easy to see that the zeroth-order term must vanish since

$$\det[\omega_0 \mathbb{I}] = 0 \Rightarrow \omega_0 = 0. \quad (3.9)$$

Now, taking into account that $\omega = \omega_1 T^{-1} + \dots$, we notice that the leading-order term in $\mathbb{M}/T^2 = \omega \mathbb{M}_\omega - k(\Omega/T) \mathbb{M}_\Omega$ becomes of order T^{-1} . Substituting Eq. (3.8) into Eq. (3.7),

we obtain:

$$\begin{aligned}\frac{1}{T^2}\mathbb{M} &= T^{-1}\mathbb{M}_1 + T^{-2}\mathbb{M}_2 + O(T^{-3}), \\ \mathbb{M}_1 &= \frac{\omega_1}{3}\mathbb{I} - \frac{2k\Omega \ln 2}{\pi^2} \begin{pmatrix} 0 & 0 & 1 \\ 0 & 0 & 0 \\ 1 & 0 & 0 \end{pmatrix}, \\ \mathbb{M}_2 &= \frac{\omega_2}{3}\mathbb{I} + \frac{4\omega_1 \ln 2}{\pi^2} \begin{pmatrix} 0 & \mu_H & \mu_A \\ \mu_H & 0 & \mu_V \\ \mu_A & \mu_V & 0 \end{pmatrix} - \frac{2k\Omega}{7\pi^2} \begin{pmatrix} \mu_A & \mu_V & 0 \\ \mu_V & -4\mu_A & \mu_H \\ 0 & \mu_H & \mu_A \end{pmatrix}.\end{aligned}\quad (3.10)$$

The determinant of \mathbb{M}_1 reads

$$\det(\mathbb{M}_1) = \frac{\omega_1 T^2}{27} \left(\frac{\omega_1^2}{T^2} - k^2 c_h^2 \right), \quad (3.11)$$

where

$$c_h = \frac{6 \ln 2 \Omega}{\pi^2 T}, \quad (3.12)$$

and the notation c_h introduced above is the propagation speed of the helical vortical wave in a neutral, unpolarized plasma with a conserved helical charge, see Eq. (116) in Ref. [15] for details. The solution $\omega_1 = 0$ of Eq. (3.12) corresponds to the so-called *Axial Vortical Wave*, while the solutions $\omega_1/T = \pm k c_h$ correspond to the *Helical Vortical Waves*. Notice that despite the velocity for the Axial Vortical Wave vanishing in the zeroth and first orders, this hydrodynamic mode is still a propagating excitation because the second order brings a nonzero contribution to ω . These properties will be discussed in detail below.

3.1 Helical Vortical Wave

The solutions $\omega_1/T \rightarrow \omega_{h,1}^\pm/T = \pm k c_h$ of Eq. (3.11) represent two propagating modes, corresponding to the *Helical Vortical Wave* (HVW). In order to compute the second order correction $\omega_{h,2}^\pm$ for the velocity of the vortical wave, we note that the inverse $(\mathbb{M}_1)^{-1}$ of the matrix \mathbb{M}_1 does not exist since we imposed $\det(\mathbb{M}_1) = 0$. Nevertheless, the following combination is still finite:

$$\det(\mathbb{M}_1)(\mathbb{M}_1)^{-1} = \frac{(\omega_{h,1}^\pm)^2}{9k^2} \begin{pmatrix} 1 & 0 & \pm 1 \\ 0 & 0 & 0 \\ \pm 1 & 0 & 1 \end{pmatrix}. \quad (3.13)$$

The leading-order contribution to $\det(\mathbb{M}/T^2)$ is thus given by $T^{-4}\text{tr}[\det(\mathbb{M}_1)\mathbb{M}_1^{-1}\mathbb{M}_2]$, which evaluates to

$$\frac{2(\omega_{h,1}^\pm)^2}{27T^4} \left\{ \omega_{h,2}^\pm + \frac{6k\Omega\mu_A}{7\pi^2} \left[\frac{84}{\pi^2} (\ln 2)^2 - 1 \right] \right\} = 0. \quad (3.14)$$

From the above equation, we obtain

$$\omega_{h,2}^\pm = -\frac{6k\Omega\mu_A}{7\pi^2} \left[\frac{84}{\pi^2} (\ln 2)^2 - 1 \right], \quad (3.15)$$

leading to the following extension of Eq. (3.12) for the velocity of the helical vortical wave:

$$\omega_h^\pm = \pm \frac{6 \ln 2}{\pi^2} \frac{k\Omega}{T} - \frac{6}{7\pi^2} \left[\frac{84}{\pi^2} (\ln 2)^2 - 1 \right] \frac{k\Omega\mu_A}{T^2} + O(T^{-3}). \quad [\text{Helical Vortical Wave}] \quad (3.16)$$

We see that at finite axial chemical potential μ_A , the angular velocity ω_h^\pm receives a non-reciprocal contribution that distinguishes between the helical vortical waves propagating along and opposite to the direction of vorticity.

Let us now consider the relation between the fluctuation amplitudes. Employing a high-temperature expansion similar to that in Eq. (3.8),

$$\delta\mu_\ell^{h;\pm} = \delta\mu_{\ell;0}^{h;\pm} + T^{-1}\delta\mu_{\ell;1}^{h;\pm} + \dots, \quad (3.17)$$

we get a matrix equation for the fluctuations of the chemical potentials, which also involve the first-order corrections. To zeroth order, this equation reads as follows:

$$\frac{\omega_1^{h;\pm}}{3} \begin{pmatrix} \pm 1 & 0 & -1 \\ 0 & \pm 1 & 0 \\ -1 & 0 & \pm 1 \end{pmatrix} \begin{pmatrix} \delta\mu_{V;0}^{h;\pm} \\ \delta\mu_{A;0}^{h;\pm} \\ \delta\mu_{H;0}^{h;\pm} \end{pmatrix} = 0, \quad (3.18)$$

giving us

$$\delta\mu_{A;0}^{h;\pm} = 0, \quad \delta\mu_{H;0}^{h;\pm} = \pm \delta\mu_{V;0}^{h;\pm}. \quad (3.19)$$

Therefore, in the leading order in the inverse temperature expansion, the helical vortical wave represents a coherent propagation of helical and vector charges as encoded in the relation (3.19) between the fluctuations of the corresponding potentials. In the same order, the axial charge content of the helical vortical wave is vanishing. To be explicit, we take the fluctuation amplitude $\delta\mu_{V;0}^{h;\pm} \equiv \delta\mu_{V;0}^{h;\pm}$ of the vector chemical potential to be the reference amplitude scale. Therefore, we impose that its higher-order corrections vanish, $\delta\mu_{V;i>0}^{h;\pm} = 0$.

Now, let us look at the next-to-the-leading order. We have a relation

$$\mathbb{M}_1 \begin{pmatrix} \delta\mu_{V;1}^{h;\pm} \\ \delta\mu_{A;1}^{h;\pm} \\ \delta\mu_{H;1}^{h;\pm} \end{pmatrix} + \mathbb{M}_2 \begin{pmatrix} 1 \\ 0 \\ \pm 1 \end{pmatrix} \delta\mu_{V;0}^{h;\pm} = 0, \quad (3.20)$$

which constraints the fluctuations of the chemical potentials as follows:

$$\delta\mu_{H;1}^{h;\pm} = \pm \delta\mu_{V;1}^{h;\pm} = 0, \quad \delta\mu_{A;1}^{h;\pm} = -\frac{\mu_H \pm \mu_V}{7 \ln 2} \left[\frac{84(\ln 2)^2}{\pi^2} - 1 \right] \delta\mu_{V;0}^{h;\pm}. \quad (3.21)$$

It can be seen that the first-order corrections to $\delta\mu_{V/H;1}^{h;\pm}$ are absent, which is consistent with the interpretation that the amplitudes $\delta\mu_{V/H}^\pm$ represent the relevant scale for the induced amplitude of the axial chemical potential.

Therefore, the HVW is a hydrodynamic excitation in vector and helical charges, with a slight admixture of the axial charge. In the HVW, the vector, axial, and helical chemical

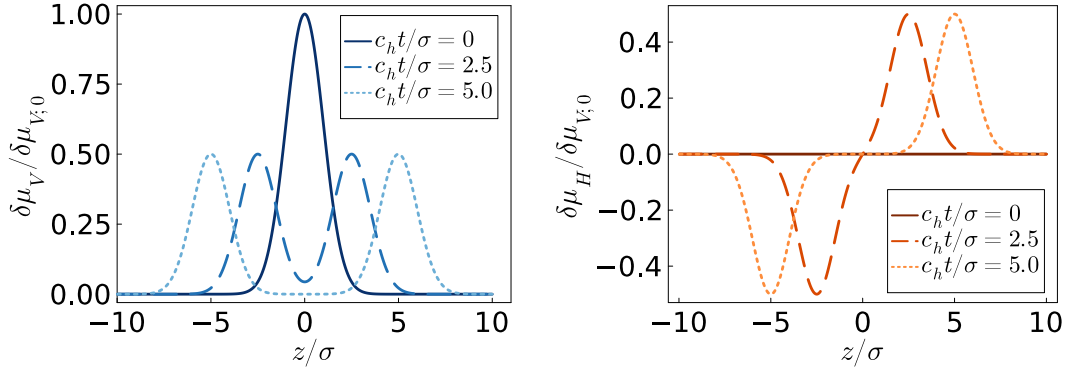


Figure 2: Time evolution of the charge perturbations (left) $\delta\bar{\mu}_V(t, z)$ and (right) $\delta\bar{\mu}_H(t, z)$, corresponding to the propagation of the helical vortical wave (HVW) through a charge-conserving plasma. The initial conditions are given in Eqs. (3.34). The background state has parameters $T = 300$ MeV, $\Omega = 6.6$ MeV, $\mu_V = 30$ MeV and $\mu_A = \mu_H = 0$, corresponding to the large temperature limit discussed in Sec. 3.

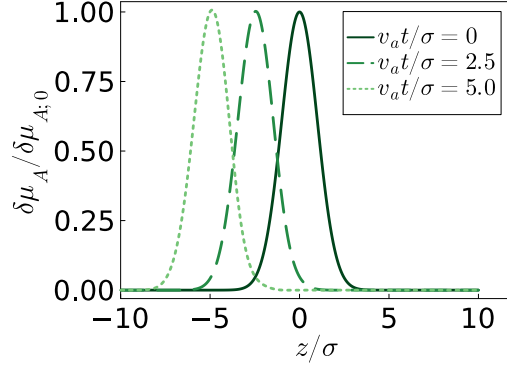


Figure 3: Time evolution of the axial charge perturbation $\delta\bar{\mu}_A(t, z)$, corresponding to the propagation of the axial vortical wave (AVW) through a charge-conserving plasma. The initial conditions are shown in Eq. (3.39). The background state has $T = 300$ MeV, $\Omega = 6.6$ MeV, $\mu_V = \mu_H = 0$ and $\mu_A = 30$ MeV, corresponding to the large temperature limit discussed in Sec. 3.

potentials are constrained as follows:

$$\begin{aligned}
\delta\mu_H^{h;\pm} &= \pm \delta\mu_V^{h;\pm}, & [\text{Helical Vortical Wave}] \\
\delta\mu_A^{h;\pm} &= -\frac{1}{7\ln 2} \left[\frac{84(\ln 2)^2}{\pi^2} - 1 \right] \frac{\mu_H \pm \mu_V}{T} \delta\mu_V^{h;\pm} + O(T^{-2}). & (3.22)
\end{aligned}$$

3.2 Axial Vortical Wave

We now focus on the axial vortical wave, for which the zeroth- and first-order terms in the angular frequency vanish, $\omega_0^a = \omega_1^a = 0$. Thus, the angular frequency reads $\omega_a =$

$\omega_2^a T^{-2} + O(T^{-3})$. In this case, we have the split

$$\begin{aligned}\mathbb{M} &= T^2 [T^{-1} \mathbb{M}_1 + T^{-2} \mathbb{M}_2 + O(T^{-3})], \\ \mathbb{M}_1 &= -\frac{2k\Omega \ln 2}{\pi^2} \begin{pmatrix} 0 & 0 & 1 \\ 0 & 0 & 0 \\ 1 & 0 & 0 \end{pmatrix}, \\ \mathbb{M}_2 &= \frac{\omega_2^a}{3} \begin{pmatrix} 1 & 0 & 0 \\ 0 & 1 & 0 \\ 0 & 0 & 1 \end{pmatrix} - \frac{2k\Omega}{7\pi^2} \begin{pmatrix} \mu_A & \mu_V & 0 \\ \mu_V & -4\mu_A & \mu_H \\ 0 & \mu_H & \mu_A \end{pmatrix}.\end{aligned}\quad (3.23)$$

At the level of the fluctuation amplitudes, the structure of \mathbb{M}_0 mandates that

$$\delta\mu_{V;0}^a = \delta\mu_{H;0}^a = 0, \quad (3.24)$$

while $\delta\mu_{A;0}^a$ remains arbitrary, and it is the relevant scale for the fluctuations in this axial wave. For the next order, we have

$$-\frac{2k\Omega \ln 2}{\pi^2} \begin{pmatrix} 0 & 0 & 1 \\ 0 & 0 & 0 \\ 1 & 0 & 0 \end{pmatrix} \begin{pmatrix} \delta\mu_{V;1}^a \\ \delta\mu_{A;1}^a \\ \delta\mu_{H;1}^a \end{pmatrix} + \left[\frac{\omega_2^a}{3} \begin{pmatrix} 1 & 0 & 0 \\ 0 & 1 & 0 \\ 0 & 0 & 1 \end{pmatrix} - \frac{2k\Omega}{7\pi^2} \begin{pmatrix} \mu_A & \mu_V & 0 \\ \mu_V & -4\mu_A & \mu_H \\ 0 & \mu_H & \mu_A \end{pmatrix} \right] \begin{pmatrix} 0 \\ \delta\mu_{A;0}^a \\ 0 \end{pmatrix} = 0. \quad (3.25)$$

The equation corresponding to the second line (which contains $\delta\mu_{A;1}^a$) can be satisfied only if the leading-order contribution to the velocity is given by

$$\omega_2^a = -\frac{24\mu_A k\Omega}{7\pi^2}. \quad (3.26)$$

The amplitude $\delta\mu_{A;1}^a$ remains unconstrained (as it should be), and without loss of generality, we set it to 0. The amplitudes corresponding to the vector and helical chemical potentials satisfy

$$\delta\mu_{V/H;1}^a = -\frac{\mu_{H/V}}{7 \ln 2} \delta\mu_{A;0}^a. \quad (3.27)$$

Restoring the inverse powers of temperature in the above equations, we arrive at the following physical picture of the Axial Vortical Wave. In the leading order, this hydrodynamic excitation is dominated by the axial chemical potential fluctuations (hence the name) $\delta\mu_A$, which is accompanied by the induced vector and helical charge densities:

$$\delta\mu_{V/H}^a = -\frac{\mu_{H/V}}{7T \ln 2} \delta\mu_A^a + O(T^{-2}), \quad [\text{Axial Vortical Wave}]. \quad (3.28)$$

In other words, the leading role in this hydrodynamic excitation is taken by the axial charge density. In the presence of the vector (helical) chemical potential, the helical (vector) chemical potential fluctuates in coherence with the axial chemical potential according to Eq. (3.28).

The axial vortical wave slowly propagates along the vorticity vector with the speed

$$v_a \equiv \frac{\omega_a}{k} = -\frac{24}{7\pi^2} \frac{\mu_A \Omega}{T^2} + O(T^{-3}), \quad [\text{Axial Vortical Wave}]. \quad (3.29)$$

The Axial Vortical Wave has three notable features. First, it propagates only in the presence of the axial background charge characterized by a nonzero axial chemical potential, $\mu_A \neq 0$. Second, the propagation has a strictly uni-directional nature (3.29): depending on the sign of the axial chemical potential, the wave propagates in the direction along (opposite to) the vorticity vector $\mathbf{\Omega}$ for $\mu_A < 0$ ($\mu_A > 0$). Third, the Axial Vortical Wave does not generate oscillations in vector and helical chemical potentials if their background values are vanishing, $\mu_V = \mu_H = 0$. In this case, the wave propagates as an oscillation in the axial chemical potential only.

3.3 Propagation properties

We now consider two concrete examples to illustrate the properties of the HVW and AVW, respectively. In the first case, we take the following initial conditions:

$$\bar{\mu}_V(t=0, z) = \mu_V + \delta\bar{\mu}_{V;0} \cos(kz), \quad \bar{\mu}_A(t=0, z) = \mu_H(t=0, z) = 0, \quad (3.30)$$

where we used the overhead bar $\bar{\mu}_V$ to denote the background value of the vector chemical potential (both the axial and helical background chemical potentials vanish). We then have three equations for the mode amplitudes,

$$\begin{aligned} \delta\mu_V^{h;+} + \delta\mu_V^{h;-} + \delta\mu_V^a &= \delta\bar{\mu}_{V;0}, \\ \delta\mu_A^{h;+} + \delta\mu_A^{h;-} + \delta\mu_A^a &= 0, \\ \delta\mu_H^{h;+} + \delta\mu_H^{h;-} + \delta\mu_H^a &= 0. \end{aligned} \quad (3.31)$$

Using Eq. (3.27), it can be seen that $\delta\mu_V^a = 0$. Using the last two of the above relations, it can be shown that $\delta\mu_A^a = 0$, which leads to the solution

$$\delta\mu_V^{h;+} = \delta\mu_V^{h;-} = \frac{1}{2}\delta\bar{\mu}_{V;0}, \quad (3.32)$$

while $\delta\mu_H^{h;\pm} = \pm\delta\mu_V^{h;\pm}$ and $\delta\mu_A^{h;\pm} = 0$, with $\delta\mu_V^a = \delta\mu_A^a = \delta\mu_H^a = 0$. The full solution describes the propagation of the helical vortical wave in an unpolarized plasma,

$$\bar{\mu}_V(t, z) = \mu_V + \delta\bar{\mu}_{V;0} \cos(kc_h t) \cos(kz), \quad \bar{\mu}_H(t, z) = \delta\bar{\mu}_{V;0} \sin(kc_h t) \sin(kz), \quad (3.33)$$

while $\bar{\mu}_A(t, z) = 0$.

We now consider the Gaussian example suggested in Eq. (2.48). We take

$$\bar{\mu}_V(0, z) = \mu_V + \delta\bar{\mu}_{V;0} e^{-z^2/2\sigma^2}, \quad \bar{\mu}_A(0, z) = \bar{\mu}_H(0, z) = 0. \quad (3.34)$$

Applying Eq. (2.49), the mode amplitudes can be found as

$$\delta\mu_V^{h;+}(k) = \delta\mu_V^{h;-}(k) = \frac{\sigma \delta\bar{\mu}_{V;0}}{2\sqrt{2\pi}} e^{-\sigma^2 k^2/2}, \quad (3.35)$$

while $\delta\mu_H^{h;\pm}(k) = \pm\delta\mu_V^{h;\pm}(k)$. Reconstituting the time-dependent profile using Eq. (2.50), we find

$$\begin{aligned} \delta\bar{\mu}_V(t, z) &= \frac{\delta\bar{\mu}_{V;0}}{2} \left[e^{-(z-c_h t)^2/2\sigma^2} + e^{-(z+c_h t)^2/2\sigma^2} \right], \\ \delta\bar{\mu}_H(t, z) &= \frac{\delta\bar{\mu}_{V;0}}{2} \left[e^{-(z-c_h t)^2/2\sigma^2} - e^{-(z+c_h t)^2/2\sigma^2} \right]. \end{aligned} \quad (3.36)$$

The HVW splits the initial Gaussian in two lumps travelling along and opposite to the vorticity vector. The excess vector charge is carried symmetrically in both directions. The lump travelling in the direction of the vorticity vector has equal vector and helicity charges, while the lump travelling opposite to the vorticity vector presents vector and helicity charges of equal magnitude but opposite sign. Thus, the HVW generates a local helicity imbalance that propagates out towards the system edges. This behaviour is illustrated in Fig. 2.

To illustrate the properties of the axial vortical wave, we set the initial conditions

$$\bar{\mu}_A(0, z) = \mu_A + \delta\bar{\mu}_{A;0} \cos(kz), \quad \bar{\mu}_H(0, z) = -\frac{\mu_V}{7T \ln 2} \delta\bar{\mu}_{A;0} \cos(kz), \quad (3.37)$$

while $\bar{\mu}_V(0, z) = \mu_V$. Then, the HVW modes vanish, $\delta\mu_\ell^{h;\pm} = 0$, for all $\ell \in \{V, A, H\}$. Moreover, $\delta\mu_V^a = 0$, while $\delta\mu_H^a = -\mu_V \delta\bar{\mu}_{A;0} / (7T \ln 2)$. The full solution reads

$$\bar{\mu}_A(t, z) = \mu_A + \delta\bar{\mu}_{A;0} \cos(\omega_a t - kz), \quad \bar{\mu}_H(t, z) = -\frac{\mu_V \delta\bar{\mu}_{A;0}}{7T \ln 2} \cos(\omega_a t - kz), \quad (3.38)$$

where $\omega_a = kv_a \simeq -24\mu_A k \Omega / (7\pi^2 T^2)$. Contrary to the solution in Eq. (3.33), the AVW is not a standing wave. It is rather a propagating solution, transferring axial charge in the direction opposite to that of the vorticity. This feature is better seen when considering the Gaussian example, with the following initial configuration:

$$\bar{\mu}_V(0, z) = \mu_V, \quad \bar{\mu}_A(0, z) = \mu_A + \delta\bar{\mu}_A e^{-z^2/2\sigma^2}, \quad \bar{\mu}_H(0, z) = -\frac{\mu_V}{7T \ln 2} \bar{\mu}_A(0, z). \quad (3.39)$$

Since only the axial mode is excited by these initial conditions, the solution trivially reads

$$\bar{\mu}_A(t, z) = \mu_A + \delta\bar{\mu}_A e^{-(z-v_a t)^2/2\sigma^2}, \quad (3.40)$$

while $\bar{\mu}_V(t, z) = \mu_V$ and $\bar{\mu}_H(t, z) = -\mu_V \bar{\mu}_A(t, z) / (7T \ln 2)$. The above solution shows clearly that the AVW will lead to uni-directional transport of the excess axial charge in the direction opposite to the vorticity. This behaviour is illustrated in Fig. 3.

3.4 Symmetries of the helical and axial vortical waves

Qualitatively, the emergence of the non-reciprocal propagation effects can be understood on the basis of discrete $\mathcal{CP}\mathcal{T}$ symmetries of the quantities involved in the process (summarized in Table 1). For a slowly rotating fluid of massless fermions, the leading contribution to the velocity of a hydrodynamic wave excitation in a rotating fluid should be linearly proportional to the magnitude of the corresponding angular velocity, $v \propto \Omega$ (here, we remove all indices for simplicity). One can also notice the collinearity of these vectors $\mathbf{v} \parallel \boldsymbol{\Omega}$ following from the spatial symmetries of the system. One gets for the dispersion relation the following generic expression:

$$\omega = C(T, \mu_V, \mu_A, \mu_H) \mathbf{k} \cdot \boldsymbol{\Omega}, \quad (3.41)$$

where C is a function of all parameters of the system.

Consider first a neutral fluid with vanishing chemical potentials, $\vec{\mu} = 0$. Since temperature T is the only dimensionful parameter in this case, one has $C \propto 1/T$ for dimensional

reasons. The latter statement also implies that C is a \mathcal{P} - and \mathcal{T} -even quantity in a neutral fluid.

The \mathcal{T} symmetries of the two sides of Eq. (3.41) are different: while the wave velocity v is a \mathcal{P} -odd quantity, the angular velocity Ω is \mathcal{P} -even (*c.f.* Table 1). Equation (3.41) is preserved under the time reversal \mathcal{T} and the charge conjugation \mathcal{C} transformations, while it changes the sign under the parity inversion \mathcal{P} .

Now we notice that in the discussed system, all chemical potentials vanish, thus implying that its \mathcal{P} - (and \mathcal{T})-symmetries are unbroken. Therefore, a \mathcal{P} transformation applied to the system should give us a system with identical properties. The latter statement is formally inconsistent with the \mathcal{P} -property of Eq. (3.41) as the parity transform—corresponding to the inversion of all spatial coordinates—flips the sign of this equation. Therefore, the wave is either absent ($C = 0$), or there are two identical waves, with $C \rightarrow \pm|C|$, propagating in opposite directions with the same velocities. These branches of Eq. (3.41) are then mapped to each other by the \mathcal{P} transformation, and the system maintains the invariance under parity transformation. The latter property, indeed, is realized in our case of the Helical Vortical Waves, indicating the reciprocity of the hydrodynamic spectrum of the neutral fluid.

Can the generic law (3.41) describe non-reciprocal waves? To figure this out, let us consider the system with all three chemical potentials non-vanishing. One can write for the proportionality function (3.41)

$$C(T, \vec{\mu}) = Tc_T + \mu_V c_V + \mu_A c_A + \mu_H c_H + \mu_V \mu_A c_{VA} + \mu_V \mu_H c_{VH} + \mu_A \mu_H c_{AH}, \quad (3.42)$$

where c_T , c_ℓ and $c_{\ell, \ell'}$ with $\ell, \ell' = V, A, H$ are \mathcal{CPT} -invariant functions of the temperature T and the chemical potentials $\vec{\mu} = (\mu_V, \mu_A, \mu_H)$.

We require that the \mathcal{C} symmetry of the system should be unbroken to be consistent with the anticipations in quantum field theory. In our case, this statement means that the spectrum of the hydrodynamic excitations in the system with particles and the identical system made of anti-particles should be the same. Since μ_V and μ_H are \mathcal{C} -odd quantities the corresponding coefficients must vanish in Eq. (3.42): $c_V = c_H = c_{VA} = c_{AH} = 0$. Therefore, we are only left with two terms in the generic expression for the group velocity:

$$\mathbf{v} = \frac{d\omega}{d\mathbf{k}} = c_T T \boldsymbol{\Omega} + c_A \mu_A \boldsymbol{\Omega} + c_{VH} \mu_V \mu_H \boldsymbol{\Omega}, \quad (3.43)$$

where we remind that c_T , c_A and c_{VH} are \mathcal{CPT} -invariant quantities.

As we discussed above, the first term in Eq. (3.43) breaks parity \mathcal{P} inversion for the hydrodynamic wave, leading to the existence of two identical counter-propagating branches that preserve reciprocity of the system. The second and the third terms do not break any symmetry since the combinations $\mu_A \boldsymbol{\Omega}$ and $\mu_V \mu_H \boldsymbol{\Omega}$ have the same \mathcal{CPT} properties as the velocity \mathbf{v} (μ_A and the product $\mu_V \mu_H$ share identical \mathcal{CPT} symmetries). Thus, the last two terms describe a wave excitation that can have no reciprocal partner.

Thus, the non-reciprocity effects appear in the presence of the finite axial chemical potential (for a chirally imbalanced fluid with $\mu_A \neq 0$), as well as in helically imbalanced ($\mu_H \neq 0$) dense ($\mu_V \neq 0$) fluid. In the lowest order in chemical potentials, the second term

in Eq. (3.43) provides a leading contribution to the non-reciprocal effects. This term enters the velocities of the helical (3.16) and axial (3.29) vortical waves.

We conclude that in the chirally imbalanced rotating fluid, the non-reciprocal gapless waves can appear in the hydrodynamic spectrum.

4 Unpolarized Plasma

We now consider the limit when the background state is unpolarized, such that $\mu_A = \mu_H = 0$. This limit is particularly relevant in realistic plasmas, when the axial and helical charge conservation is broken by interactions (see companion paper [26]). We refer to this case as the *unpolarized* plasma.

Setting $\mu_A = \mu_H = 0$ in Eq. (2.10) leads to

$$P = -\frac{T^4}{\pi^2} \sum_{\sigma,\lambda} \text{Li}_4(e^{\sigma\mu_V/T}) = \frac{7\pi^2 T^4}{180} + \frac{\mu_V^2 T^2}{6} + \frac{\mu_V^4}{12\pi^2}, \quad (4.1)$$

where we used Eq. (5.2) to eliminate the polylogarithms. The charge densities Q_ℓ can be computed by differentiating the pressure P in Eq. (2.10) with respect to the corresponding chemical potential μ_ℓ , as shown in Eq. (2.11), using the property

$$\frac{\partial}{\partial \mu_\ell} \text{Li}_n(-e^{\mu_{\sigma,\lambda}/T}) = \frac{q_{\sigma,\lambda}^\ell}{T} \text{Li}_{n-1}(-e^{\mu_{\sigma,\lambda}/T}). \quad (4.2)$$

This leads to

$$Q_\ell = -\frac{T^3}{\pi^2} \sum_{\sigma,\lambda} q_{\sigma,\lambda}^\ell \text{Li}_3(e^{\sigma\mu_V/T}) = \delta_{\ell,V} \left(\frac{\mu_V T^2}{3} + \frac{\mu_V^3}{3\pi^2} \right), \quad (4.3)$$

where we have used the properties $\sum_{\sigma,\lambda} q_{\sigma,\lambda} = 0$ (thus, Q_A and Q_H vanish), as well as

$$\text{Li}_3(-e^\alpha) - \text{Li}_3(-e^{-\alpha}) = -\frac{\pi^2 \alpha}{6} - \frac{\alpha^3}{6}. \quad (4.4)$$

Since $Q_A = 0$, the Landau-frame vortical conductivities $\sigma_\ell^\omega = \sigma_{\ell;\beta}^\omega - Q_A Q_\ell / (E + P)$ agree with the β -frame ones, $\sigma_\ell^\omega = \sigma_{\ell;\beta}^\omega = \frac{1}{2} \partial^2 P / \partial \mu_A \partial \mu_\ell$. The second derivatives of the pressure with respect to the chemical potentials can be evaluated as

$$\frac{\partial^2 P}{\partial \mu_\ell \partial \mu_{\ell'}} = \frac{\partial Q_\ell}{\partial \mu_{\ell'}} = -\frac{T^2}{\pi^2} \sum_{\sigma,\lambda} q_{\sigma,\lambda}^\ell q_{\sigma,\lambda}^{\ell'} \text{Li}_2(-e^{\mu_{\sigma,\lambda}/T}) = 2 \begin{pmatrix} \sigma_A^\omega & 0 & 0 \\ 0 & \sigma_A^\omega & \sigma_H^\omega \\ 0 & \sigma_H^\omega & \sigma_A^\omega \end{pmatrix}, \quad (4.5)$$

where we used Eq. (1.1) and $q_\ell^2 = 1$ to simplify the product $q_{\sigma,\lambda}^\ell q_{\sigma,\lambda}^{\ell'}$ of two charges. The vector vortical conductivity $\sigma_V^\omega = \frac{1}{2} \partial^2 P / \partial \mu_V \partial \mu_A$ involves the product $q_{\sigma,\lambda}^V q_{\sigma,\lambda}^A = q_{\sigma,\lambda}^H = 2\lambda\sigma$ and hence vanishes. The axial conductivity is given by

$$\sigma_A^\omega = -\frac{T^2}{2\pi^2} \sum_{\sigma,\lambda} \text{Li}_2(-e^{\sigma\mu_V/T}) = \frac{T^2}{6} + \frac{\mu_V^2}{2\pi^2}, \quad (4.6)$$

where we used the following property of the polylogarithm function:

$$\text{Li}_2(-e^a) + \text{Li}_2(-e^{-a}) = -\frac{\pi^2}{6} - \frac{a^2}{2}. \quad (4.7)$$

The helical vortical conductivity can be expressed as

$$\sigma_H^\omega = \frac{T^2}{\pi^2} [\text{Li}_2(-e^{-\mu_V/T}) - \text{Li}_2(-e^{\mu_V/T})], \quad (4.8)$$

and reduces for small and large $|\mu_V/T|$ to:

$$\begin{aligned} \sigma_H^\omega(|\mu_V| \ll T) &= \frac{2 \ln 2}{\pi^2} T \mu_V + O(T^{-1}), \\ \sigma_H^\omega(|\mu_V| \gg T) &\simeq \text{sgn}(\mu_V) \left[\sigma_A^\omega - \frac{2T^2}{\pi^2} e^{-|\mu_V|/T} + O(e^{-2|\mu_V|/T}) \right]. \end{aligned} \quad (4.9)$$

Finally, we need to consider the derivatives of the vortical charge conductivities $\sigma_\ell^\omega = \sigma_{\ell;\beta}^\omega - Q_A Q_\ell / (E + P)$ with respect to the chemical potential. Here, the second term makes a non-vanishing contribution since $\partial Q_A / \partial \mu_{\ell'} = 2\sigma_{\ell'}^\omega$:

$$\frac{\partial}{\partial \mu_{\ell'}} \left(\frac{Q_A Q_\ell}{E + P} \right)_{\mu_A = \mu_H = 0} = \frac{2Q_V \sigma_{\ell'}^\omega}{E + P} \delta_{\ell V}. \quad (4.10)$$

The derivative of the β -frame vortical conductivity evaluates to

$$\frac{\partial \sigma_{\ell;\beta}^\omega}{\partial \mu_{\ell'}} = \frac{1}{2} \frac{\partial^3 P}{\partial \mu_{\ell'} \partial \mu_A \partial \mu_\ell} = \frac{1}{\pi^2} \begin{pmatrix} 0 & \mu_V & TL \\ \mu_V & 0 & 0 \\ TL & 0 & 0 \end{pmatrix}, \quad (4.11)$$

where we introduced the notation L based on the relations

$$\begin{aligned} \text{Li}_1(-e^{\mu_V/T}) - \text{Li}_1(-e^{-\mu_V/T}) &= -\frac{\mu_V}{T}, \\ L = -\frac{1}{T} \left[\text{Li}_1(-e^{\mu_V/T}) + \text{Li}_1(-e^{-\mu_V/T}) \right] &= 2 \ln \left(2 \cosh \frac{\mu_V}{2T} \right), \end{aligned} \quad (4.12)$$

taking into account that $\text{Li}_1(-e^\alpha) = -\ln(1 + e^\alpha)$. As with σ_H^ω , the degenerate limit for L involves an exponentially-decaying function. For convenience, we list below both the high-temperature and the large-chemical potential limits:

$$\begin{aligned} L(T \gg |\mu_V|) &= 2 \ln 2 + \frac{\mu_V^2}{4T^2} - \frac{\mu_V^4}{96T^4} + O\left(\frac{\mu_V^6}{T^6}\right), \\ L(|\mu_V| \gg T) &= \frac{|\mu_V|}{T} + 2e^{-|\mu_V|/T} + \dots, \end{aligned} \quad (4.13)$$

where we suppressed terms that decay faster than $e^{-|\mu_V|/T}$. We thus conclude that

$$\frac{\partial \sigma_\ell^\omega}{\partial \mu_{\ell'}} = -\delta_{\ell V} \frac{2Q_V \sigma_{\ell'}^\omega}{E + P} + \frac{1}{\pi^2} \begin{pmatrix} 0 & \mu_V & TL \\ \mu_V & 0 & 0 \\ TL & 0 & 0 \end{pmatrix}. \quad (4.14)$$

Once again, we have to find the non-trivial solutions of the system (2.33). As in the previous subsection, let us define the dimensionless chemical potential $\alpha_V = \mu_V/T$. Then the matrix \mathbb{M} has the following structure:

$$\frac{1}{T^2}\mathbb{M} = \omega\mathbb{M}_\omega(\alpha_V) - \frac{k\Omega}{T}\mathbb{M}_\Omega(\alpha_V), \quad (4.15)$$

with \mathbb{M}_ω and \mathbb{M}_Ω given by

$$\mathbb{M}_\omega = \frac{2}{T^2} \begin{pmatrix} \sigma_A^\omega - \frac{T^2}{3}\Delta H & 0 & 0 \\ 0 & \sigma_A^\omega & \sigma_H^\omega \\ 0 & \sigma_H^\omega & \sigma_A^\omega \end{pmatrix}, \quad \mathbb{M}_\Omega = \begin{pmatrix} 0 & \frac{1}{H}A & \frac{1}{H}B \\ A & 0 & 0 \\ B & 0 & 0 \end{pmatrix}, \quad (4.16)$$

where $\Delta H = H - 1$ with $H = (e + P)/sT = 1 + \mu_V Q_V/(sT)$, while A and B are defined as

$$A = \frac{\alpha_V}{\pi^2} - \frac{Q_V}{3s}, \quad B = \frac{HL}{\pi^2} - \frac{2Q_V}{sT^2}\sigma_H^\omega. \quad (4.17)$$

Since $\det(\mathbb{M}_1) = 0$, one can conclude that $\det(\mathbb{M}) = 0$ has $\omega_0 = 0$ as a solution. This non-propagating mode is a fluctuation in a purely axial-helical sector, i.e. $\delta\mu_V^0 = 0$, with the axial and helical fluctuations being related as follows:

$$A\delta\mu_A^0 + B\delta\mu_H^0 = 0. \quad (4.18)$$

The other two modes correspond to the helical vortical wave. Their angular frequencies satisfy the following equation:

$$\omega_h^2 \left(\frac{2}{T^2}\right)^2 \left(\sigma_A^\omega - \frac{T^2}{3}\Delta H\right) [(\sigma_A^\omega)^2 - (\sigma_H^\omega)^2] - \frac{k^2\Omega^2}{HT^2} [\sigma_A^\omega(A^2 + B^2) - 2AB\sigma_H^\omega] = 0. \quad (4.19)$$

There are two solution branches:

$$\omega_h^\pm = \pm \frac{k\Omega T}{2} \sqrt{\frac{\sigma_A^\omega(A^2 + B^2) - 2AB\sigma_H^\omega}{H(\sigma_A^\omega - \frac{T^2}{3}\Delta H)[(\sigma_A^\omega)^2 - (\sigma_H^\omega)^2]}}. \quad (4.20)$$

The above solution is completely analytical, allowing the large temperature and degenerate limits to be taken explicitly. At high temperature, we have

$$\begin{aligned} \sigma_A^\omega &= \frac{T^2}{6} + \frac{\mu_V^2}{2\pi^2}, & \sigma_H^\omega &= \frac{2\ln 2}{\pi^2}T^2\alpha_V + O(\alpha_V^3), & H &= 1 + \frac{15\alpha_V^2}{7\pi^2} + O(\alpha_V^4), \\ L &= 2\ln 2 + O(\alpha_V^2), & A &= \frac{2\alpha_V}{7\pi^2} + O(\alpha_V^3), & B &= \frac{2\ln 2}{\pi^2} + \frac{7\pi^2 - 120\ln 2}{28\pi^4}\alpha_V^2 + O(\alpha_V^4). \end{aligned} \quad (4.21)$$

It can be seen that the axial vortical conductivity σ_A dominates over its helical counterpart σ_H , such that to leading order, $\omega_h^\pm \simeq \pm(k\Omega T/2) \times (B/\sigma_A) \simeq \pm kc_h$, with c_h being the speed of the helical vortical wave given in Eq. (3.12). Taking into account terms up to next-to-leading order, we arrive at the following expression for the helical vortical wave:

$$\omega_h^\pm(T \gg |\mu_V|) = \pm \frac{k\Omega}{T} \left[\frac{6\ln 2}{\pi^2} - 0.0124 \frac{\mu_V^2}{T^2} + O(\mu_V^4/T^4) \right]. \quad (4.22)$$

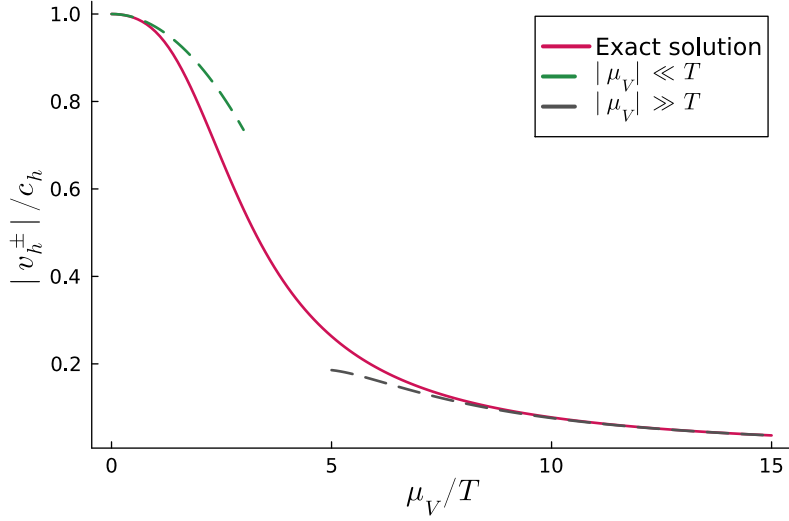


Figure 4: Phase velocity $v_h^\pm = \omega_h^\pm/k$ of the helical vortical wave as a function of μ_V/T , for the unpolarized plasma in which the background axial and helical densities are vanishing ($\mu_A = \mu_H = 0$). The result is normalized to the speed of the HVW in the neutral plasma, $c_h = \frac{6 \ln 2 \Omega}{\pi^2} \frac{\Omega}{T} \simeq 0.42 \frac{\Omega}{T}$.

In the limit of vanishing chemical potentials for the neutral plasma, Eq. (4.22) coincides with Eq. (3.16).

In the opposite limit of large chemical potential, we have $\sigma_A^\omega - s_V \sigma_H^\omega = (2T^2/\pi^2)e^{-|\mu_V|/T}$, where we abbreviated $s_V = \text{sgn}(\mu_V)$. Thus, we can replace

$$(\sigma_A^\omega)^2 - (\sigma_H^\omega)^2 = \frac{4T^2}{\pi^2} \sigma_A^\omega e^{-|\mu_V|/T}. \quad (4.23)$$

The numerator of the fraction appearing under the square root in Eq. (4.20) can be put in the form

$$\sigma_A^\omega(A^2 + B^2) - 2AB\sigma_H^\omega = \sigma_A^\omega(A - s_V B)^2 + \frac{4s_V T^2}{\pi^2} AB e^{-|\mu_V|/T}. \quad (4.24)$$

The first term of the right-hand side of the above equation becomes subleading due to the asymptotic relation

$$B \simeq s_V A + \frac{2}{\pi^2} \left(H + \frac{2s_V Q_V}{s} \right) e^{-|\mu_V|/T}. \quad (4.25)$$

Taking into account that

$$H = \frac{\alpha_V^2}{\pi^2} \left(1 + \frac{23\pi^2}{15\alpha_V^2} + O(\alpha_V^{-4}) \right), \quad A = \frac{2\alpha_V}{3\pi^2} \left(1 - \frac{4\pi^2}{15\alpha_V^2} + O(\alpha_V^{-4}) \right),$$

$$\frac{2s_V Q_V}{s} = \frac{2s_V}{\alpha_V} (H - 1) \simeq \frac{2s_V \alpha_V}{\pi^2} \left(1 + \frac{8\pi^2}{15\alpha_V^2} + O(\alpha_V^{-4}) \right), \quad (4.26)$$

we finally arrive at

$$\omega_h^\pm = \pm \frac{k\Omega A \sqrt{3}}{2\sqrt{H\sigma_A^\omega \left(\frac{3}{T^2} \sigma_A^\omega - \Delta H \right)}} + O(e^{-|\mu_V|/T}). \quad (4.27)$$

Expanding the above in powers of T/μ_V , we get

$$\omega_h^\pm(|\mu_V| \gg T) = \pm \frac{2\pi k \Omega T}{\mu_V^2 \sqrt{3}} \left[1 - \frac{7\pi^2 T^2}{6\mu_V^2} + O\left(\frac{T^4}{\mu_V^4}\right) \right]. \quad (4.28)$$

We display the phase velocity of the Helical Vortical Wave $v_h^\pm = \omega_h^\pm/k$ normalized to the neutral plasma velocity $c_h = 6\Omega \ln 2/\pi^2 T$ in Figure 4. The quantity $|v_h^\pm|$ exhibits a monotonically-decreasing dependence on $\alpha_V = \mu_V/T$. We also display using dotted lines the asymptotic limits for large temperature and large chemical potential, shown in Eqs. (4.22) and (4.28), respectively.

The explicit space-time solutions as standing waves or as the evolution of the Gaussian initial state shown in Eqs. (3.33) and (3.36) apply straightforwardly to the case considered here by replacing the velocity $\pm c_h$ of the HVW in a neutral plasma with ω_h^\pm/k given in Eq. (4.20).

Summarizing, the unpolarized ($\mu_A = \mu_H = 0$) plasma maintains only the Helical Vortical Wave, while its axial vortical analogue is absent since the background axial density vanishes. The finite vector chemical potential μ_V results in slowing down the propagation of the Helical wave, as indicated in Fig. 4 and confirmed by the asymptotic results in Eqs. (4.22) and (4.28).

5 Degenerate limit of high-density matter and non-reciprocity

We now consider the case when the fermion gas is strongly degenerate, i.e., when the vector charge density is higher than any other scales in the system so that $|\mu_V| \gg T, |\mu_A|, |\mu_H|$. We analyze this system by rewriting the pressure (2.10) as follows:

$$P = -\frac{T^4}{\pi^2} \sum_\lambda \left[\text{Li}_4\left(-e^{\alpha_V + 2\lambda(\alpha_H + \alpha_A)}\right) + \text{Li}_4\left(-e^{-\alpha_V + 2\lambda(\alpha_A - \alpha_H)}\right) \right], \quad (5.1)$$

where we denoted the dimensionless chemical potentials $\alpha_\ell = \mu_\ell/T$. We now wish to eliminate the polylogarithms using the relation

$$\text{Li}_4(-e^\alpha) + \text{Li}_4(-e^{-\alpha}) = -\frac{7\pi^4}{360} - \frac{\pi^2 \alpha^2}{12} - \frac{\alpha^4}{24}. \quad (5.2)$$

The arguments of the exponentials in the polylogarithms appearing in Eq. (5.1) are, however, not balanced as required in Eq. (5.2). To apply this formula, we first rewrite Eq. (5.1) as

$$P = -\frac{T^4}{\pi^2} \sum_\lambda \left[\text{Li}_4(-e^{|\alpha_V| + 2\lambda(\alpha_A + s_V \alpha_H)}) + \text{Li}_4(-e^{-|\alpha_V| + 2\lambda(\alpha_A - s_V \alpha_H)}) \right], \quad (5.3)$$

where $s_V = \text{sgn}(\alpha_V)$ represents the sign of the vector chemical potential. Taking into account the explicit expression of the polylogarithm,

$$\text{Li}_n(z) = \sum_{j=1}^{\infty} \frac{z^j}{j^n} = z + \frac{z^2}{2^n} + O(z^3), \quad (5.4)$$

we seek to eliminate the polylogarithms whose arguments contain the $e^{|\alpha_V|}$ factor by adding and subtracting the term $\text{Li}_4(-e^{-|\alpha_V|-2\lambda(\alpha_A+s_V\alpha_H)})$. Taking only the first term in Eq. (5.4), we see that these added terms behave as $\sim e^{-|\alpha_V|}$ at large α_V , and are therefore exponentially suppressed.

Writing $P = \tilde{P} + P_e$, we collect in \tilde{P} the terms obtained by pairing the polylogarithms as in Eq. (5.2) and in P_e the remaining non-essential terms, which are exponentially suppressed:

$$\begin{aligned}\tilde{P} &= -\frac{T^4}{\pi^2} \sum_{\sigma,\lambda} \text{Li}_4\left(-e^{\sigma|\alpha_V|+2\lambda\sigma(\mu_A+s_V\mu_H)}\right) \\ &= \frac{7\pi^2 T^4}{180} + \frac{T^2}{6}(\mu_V^2 + \mu_\chi^2) + \frac{1}{12\pi^2}(\mu_V^4 + 6\mu_V^2\mu_\chi^2 + \mu_\chi^4), \\ P_e &= -\frac{T^4}{\pi^2} \sum_{\sigma,\lambda} \sigma \text{Li}_4(-e^{-|\alpha_V|-2\lambda s_V\alpha_H+2\lambda\sigma\alpha_A}) \simeq -\frac{4T^4}{\pi^2} e^{-|\alpha_V|} \sinh\alpha_A \sinh\alpha_H,\end{aligned}\quad (5.5)$$

where $\sigma = \pm 1$ was introduced for compactness. It can be seen that the chemical potentials μ_A and μ_H enter the dominant part of the pressure \tilde{P} only through the symmetric combination

$$\mu_\chi = \mu_A + s_V\mu_H. \quad (5.6)$$

For later convenience, we also introduce the conjugate combination,

$$\mu_{\tilde{\chi}} = \mu_A - s_V\mu_A, \quad (5.7)$$

For the purpose of studying the excitations in the degenerate limit, we neglect the exponentially damped contributions coming from P_e . We will restore these terms later in this section. Using the standard machinery described in Sec. 2.2, we can derive the charge densities, entropy density, and the β - and Landau-frame vortical conductivities, as follows:

$$\begin{aligned}\tilde{Q}_V &= \frac{\mu_V T^2}{3} + \frac{\mu_V^3 + 3\mu_V\mu_\chi^2}{3\pi^2}, & \tilde{Q}_\chi &= \frac{\mu_\chi T^2}{3} + \frac{\mu_\chi^3 + 3\mu_V^2\mu_\chi}{3\pi^2}, \\ \tilde{s} &= \frac{7\pi^2 T^3}{45} + \frac{T}{3}(\mu_V^2 + \mu_\chi^2), & \tilde{\sigma}_{V;\beta}^\omega &= \frac{\mu_V\mu_\chi}{\pi^2}, & \tilde{\sigma}_{\chi;\beta}^\omega &= \frac{T^2}{6} + \frac{\mu_V^2 + \mu_\chi^2}{2\pi^2}, \\ \tilde{\sigma}_V^\omega &= \tilde{\sigma}_{V;\beta}^\omega - \frac{\tilde{Q}_\chi\tilde{Q}_V}{4\tilde{P}}, & \tilde{\sigma}_\chi^\omega &= \tilde{\sigma}_{\chi;\beta}^\omega - \frac{\tilde{Q}_\chi^2}{4\tilde{P}}\end{aligned}\quad (5.8)$$

where $\tilde{Q}_\chi = \tilde{Q}_A = s_V\tilde{Q}_H$ and $\tilde{\sigma}_{\chi;\beta}^\omega = \tilde{\sigma}_{A;\beta}^\omega = s_V\tilde{\sigma}_{H;\beta}^\omega$. It can be seen that the axial charge density and vortical conductivity are equal to the helical ones multiplied by the sign $s_V = \text{sgn}(\mu_V)$ of the vector chemical potential μ_V because, for an ensemble of single-charge particles (as dictated by the high vector potential), the total helical and axial charges are equal to each other up to s_V . Due to this reason, the lines corresponding to $\ell = A$ and H , as well as the columns corresponding to $\ell' = A$ and H , are proportional to each other at the level of the non-exponential part of the matrix $\tilde{\mathbb{M}}_{\ell\ell'}$, i.e.

$$\tilde{\mathbb{M}}_{A\ell'} = s_V\tilde{\mathbb{M}}_{H\ell'}, \quad \tilde{\mathbb{M}}_{\ell A} = s_V\tilde{\mathbb{M}}_{\ell H}. \quad (5.9)$$

The above observation implies that, in the strongly degenerate regime, the oscillations in the helical and axial chemical are additive, providing only one degree of freedom in the

form $\delta\mu_\chi = \delta\mu_A + s_V\delta\mu_H$. As we just mentioned, this property is to be expected since when the system consists only of particles (that is, there are no antiparticles present), the helicity and chirality are indistinguishable from each other and, therefore, they enter only in the combination (5.6). Due to the very same reason, at high vector density, the helical and axial vortical waves form the same hydrodynamic excitation, the Axial-Helical Vortical Wave, which inherits features from both original waves.

We now formally introduce a small parameter ε such that $T \rightarrow \varepsilon T$ and $\mu_\chi \rightarrow \varepsilon\mu_\chi$. We further consider an expansion of the velocity of the form $\omega \rightarrow \tilde{\omega} = \tilde{\omega}_0 + \tilde{\omega}_1\varepsilon + \dots$. A series expansion with respect to ε yields:

$$\begin{aligned}\tilde{\mathbb{M}}_{VV} &= \frac{\tilde{\omega}_0\mu_V^2}{3\pi^2} + \frac{\varepsilon(4\mu_\chi k\Omega + \tilde{\omega}_1\mu_V^2)}{3\pi^2} + O(\varepsilon^2), & \tilde{\mathbb{M}}_{V\chi} &= -\frac{2\varepsilon^2 k\Omega}{\mu_V} \left(\frac{T^2}{3} + \frac{2\mu_\chi^2}{\pi^2} \right) + O(\varepsilon^3), \\ \tilde{\mathbb{M}}_{\chi V} &= -\frac{2k\Omega\mu_V}{3\pi^2} + \frac{4\varepsilon\tilde{\omega}_0\mu_V\mu_\chi}{3\pi^2} + O(\varepsilon^2), & \tilde{\mathbb{M}}_{\chi\chi} &= \frac{\tilde{\omega}_0\mu_V^2}{\pi^2} + \frac{\varepsilon(6\mu_\chi k\Omega + \tilde{\omega}_1\mu_V^2)}{\pi^2},\end{aligned}\quad (5.10)$$

where $\tilde{\mathbb{M}}_{V\chi} = \tilde{\mathbb{M}}_{VA} = s_V\tilde{\mathbb{M}}_{VH}$, $\tilde{\mathbb{M}}_{\chi V} = \tilde{\mathbb{M}}_{AV} = s_V\tilde{\mathbb{M}}_{HV}$, and $\tilde{\mathbb{M}}_{\chi\chi} = \tilde{\mathbb{M}}_{AA} = s_V\tilde{\mathbb{M}}_{AH} = s_V\tilde{\mathbb{M}}_{HA} = \tilde{\mathbb{M}}_{HH}$. Taking the determinant, it can be seen that at order $O(\varepsilon^0)$, we have $\tilde{\omega}_0^2\mu_V^4/3\pi^4 = 0$, such that $\tilde{\omega}_0 = 0$ and $\tilde{\omega}$ becomes of first order with respect to ε . The next non-vanishing contribution is of order ε^2 , with the corresponding equation given by:

$$\tilde{\omega}_1^2\mu_V^4 + 10\tilde{\omega}_1\mu_\chi\mu_V^2 k\Omega + 16\mu_\chi^2 k^2\Omega^2 - \frac{4\pi^2 T^2}{3} k^2\Omega^2 = 0. \quad (5.11)$$

Solving the above equation, we obtain the energy dispersion relation of the vortical wave in the degenerate matter:

$$\tilde{\omega}_\pm = -\frac{5k\Omega\mu_\chi}{\mu_V^2} \pm \frac{k\Omega}{\mu_V^2} \sqrt{\frac{4\pi^2 T^2}{3} + 9\mu_\chi^2}, \quad [\text{Axial-Helical Vortical Wave}]. \quad (5.12)$$

The wave appears to couple fluctuations $\tilde{\delta\mu}_V$ in the vector chemical potential and the fluctuations in the combined axial-helical chemical potentials $\tilde{\delta\mu}_\chi$ as follows:

$$\tilde{\delta\mu}_V^\pm = \frac{3\tilde{\delta\mu}_\chi^\pm}{2\mu_V} \left(\mu_\chi \pm \sqrt{\frac{4\pi^2 T^2}{3} + 9\mu_\chi^2} \right), \quad [\text{Axial-Helical Vortical Wave}]. \quad (5.13)$$

Both the energy dispersion relation (5.12) and the charge density content (5.13) of the Axial-Helical Vortical Wave depend on the sum μ_χ of the axial and helical chemical potentials (5.6).

In the presence of a finite axial (or helical) charge density, the propagation of the wave becomes non-reciprocal with respect to the direction of the angular velocity $\mathbf{\Omega}$. In general, the speed of the wave $\tilde{v}_+ = \tilde{\omega}_+/k$ parallel to the direction of the angular velocity $\mathbf{\Omega}$ and the speed $\tilde{v}_- = \tilde{\omega}_-/k$ in the direction anti-parallel to $\mathbf{\Omega}$ are different from each other (5.12). For example, setting high temperature $T \gg |\mu_\chi|$ (but still maintaining the degenerate limit $\mu_V \gg T$), we clearly see from Eq. (5.12) that the wave propagates in both directions with an offset in the velocities given by the first term. For a positive (negative) sign of the product

$\mu_\chi \Omega$, the wave propagates thus faster opposite (along) the vorticity vector $|\tilde{v}_-| > |\tilde{v}_+|$ ($|\tilde{v}_-| < |\tilde{v}_+|$).

Moreover, at the critical temperature

$$T_c^{\text{deg}} = \frac{2\sqrt{3}}{\pi} |\mu_\chi|, \quad (5.14)$$

the speed of propagation of the wave along (opposite to) the vorticity vector vanishes if the product $\mu_\chi \Omega$ takes a positive (negative) value. Thus, at the critical temperature (5.14), one of the branches of the axial-helical wave is propagating (anti-)parallel to the vorticity while the other branch represents a static mode. If the temperature is below the critical value (5.14), then both modes propagate in the same direction in a transparent manifestation of non-reciprocity.

Thus, in the cold and dense rotating matter, the hydrodynamical waves propagate in a non-reciprocal manner with respect to the global angular velocity if the background state is axially or helically imbalanced. Moreover, the relation between the magnitudes of the vector and axial-helical components of the wave differs in the waves propagating in opposite directions (5.13). These properties represent a unique feature of hydrodynamic excitations possessing the helical degree of freedom.

Considering now a vector wave constructed as in Eq. (2.44), namely $\bar{\mu}_V(t=0, z) = \mu_V + \delta\bar{\mu}_{V;0} \cos(kz)$ and $\bar{\mu}_\chi(t=0, z) = \mu_\chi$, with $|\mu_V| \gg |\mu_\chi|$, we find

$$\delta\bar{\mu}_V^\pm = \frac{1}{2} \left(1 \pm \frac{\mu_\chi}{\mathfrak{s}}\right) \delta\bar{\mu}_{V;0}, \quad \delta\mu_\chi^\pm = \pm \frac{\mu_V}{3\mathfrak{s}} \delta\bar{\mu}_{V;0}, \quad (5.15)$$

with $\mathfrak{s} = \sqrt{4\pi^2 T^2/3 + 9\mu_\chi^2}$. This leads to

$$\begin{aligned} \bar{\mu}_V(t, z) &= \mu_V + \delta\bar{\mu}_{V;0} \cos\left(kz - \frac{5\Omega\mu_\chi}{\mu_V^2} kt\right) \cos\left(\frac{k\Omega t}{\mu_V^2} \mathfrak{s}\right) \\ &\quad - \frac{\mu_\chi \delta\bar{\mu}_{V;0}}{\mathfrak{s}} \sin\left(kz - \frac{5\Omega\mu_\chi}{\mu_V^2} kt\right) \sin\left(\frac{k\Omega t}{\mu_V^2} \mathfrak{s}\right), \\ \bar{\mu}_\chi(t, z) &= \mu_\chi - \frac{\mu_V \delta\bar{\mu}_{V;0}}{3\mathfrak{s}} \sin\left(kz - \frac{5\Omega\mu_\chi}{\mu_V^2} kt\right) \sin\left(\frac{k\Omega t}{\mu_V^2} \mathfrak{s}\right). \end{aligned} \quad (5.16)$$

In the case of the initial Gaussian distribution in Eq. (2.48) for the perturbation in the vector chemical potential, $\bar{\mu}_V(0, z) = \mu_V + \delta\bar{\mu}_{V;0} e^{-z^2/2\sigma^2}$, with constant $\bar{\mu}_\chi(0, z) = \mu_\chi$, we have

$$\begin{aligned} \bar{\mu}_V(t, z) &= \mu_V + \frac{\delta\bar{\mu}_{V;0}}{2} \left[\left(1 + \frac{\mu_\chi}{\mathfrak{s}}\right) e^{-(z-\tilde{v}_+t)^2/2\sigma^2} + \left(1 - \frac{\mu_\chi}{\mathfrak{s}}\right) e^{-(z-\tilde{v}_-t)^2/2\sigma^2} \right], \\ \bar{\mu}_\chi(t, z) &= \mu_\chi + \frac{\mu_V \delta\bar{\mu}_{V;0}}{3\mathfrak{s}} \left[e^{-(z-\tilde{v}_+t)^2/2\sigma^2} - e^{-(z-\tilde{v}_-t)^2/2\sigma^2} \right], \end{aligned} \quad (5.17)$$

where $\tilde{v}_\pm = -5\Omega\mu_\chi/\mu_V^2 \pm \Omega\mathfrak{s}/\mu_V^2$ represent the group velocities corresponding to the two propagating modes.

The propagation of the initial Gaussian distribution is considered in Fig. 5. For definiteness, we took a small background temperature of $T = 10$ MeV and a background vector

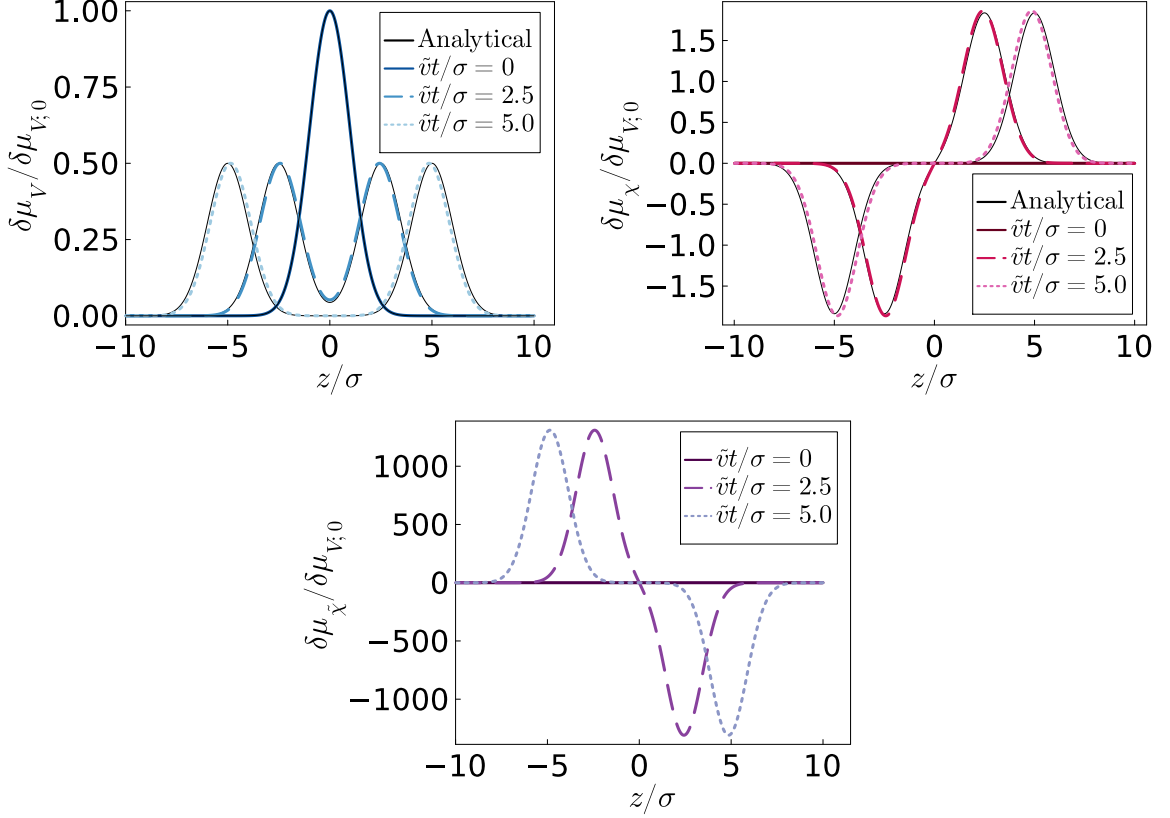


Figure 5: Time evolution of the charge perturbations (top left) $\delta\bar{\mu}_V(t, z)$, (top right) $\delta\bar{\mu}_\chi(t, z)$ and (bottom) $\delta\bar{\mu}_{\tilde{\chi}}$, corresponding to the propagation of the axial-helical vortical wave through a charge-conserving plasma. The initial conditions are given in Eqs. (3.34). The background state has parameters $T = 10$ MeV, $\Omega = 6.6$ MeV, $\mu_V = 200$ MeV and $\mu_A = \mu_H = 0$, corresponding to the degenerate limit discussed in Sec. 5. In the label, \tilde{v} is the absolute value of the corresponding speed of the wave $\tilde{v}_\pm = \tilde{\omega}_\pm/k$ defined in 5.12. The analytical solution (black) 5.17 is superimposed onto the numerical solutions (blue and pink).

chemical potential of $\mu_V = 100$ MeV, while the background axial and helical chemical potentials were set to zero. The left and middle panels demonstrate the expected analytical solution derived in Eq. (5.17). Surprisingly, the third panel reveals that the combination $\delta\bar{\mu}_{\tilde{\chi}} = \delta\bar{\mu}_A - s_V\delta\bar{\mu}_H$ grows to very high values. In the degenerate limit described by the tilde quantities (e.g., \tilde{P}) in Eq. (5.10), the combination $\delta\bar{\mu}_{\tilde{\chi}}$ is not accessible.

To understand this behaviour described above, we move back to the unpolarized plasma considered in Sec. 4 and derive the relation between all mode amplitudes before taking the degenerate limit. Considering the exact expression for the matrices \mathbb{M}_ω and \mathbb{M}_Ω in Eq. (4.16), we can find the relations between the amplitudes corresponding to the trivial

mode $\omega_0 = 0$ as follows:

$$\delta\mu_V^0 = 0, \quad \delta\mu_{\tilde{\chi}}^0 = -\frac{A + s_V B}{A - s_V B} \delta\mu_{\tilde{\chi}}^{\text{im.}} \simeq -\frac{2\pi^2}{3|\alpha_V|} e^{|\alpha_V|} \delta\mu_{\tilde{\chi}}^0. \quad (5.18)$$

Clearly, exciting the $\delta\mu_{\tilde{\chi}}^0$ amplitude leads to an exponentially-larger amplitude $\delta\mu_{\tilde{\chi}}^0$.

In the case of the non-trivial (helical) modes, when ω_h^\pm is given by Eq. (4.20), we can take the amplitude of the vector charge fluctuation, $\delta\mu_V^{h;\pm}$, as the reference amplitude. The amplitudes $\delta\mu_{\tilde{\chi}}^{h;\pm}$ and $\delta\mu_{\tilde{\chi}}^{h;\pm}$ are then given by

$$\begin{aligned} \delta\mu_{\tilde{\chi}}^{h;\pm} &= \frac{k\Omega T}{2\omega_h^\pm} \frac{A + s_V B}{\sigma_A^\omega + s_V \sigma_H^\omega} \delta\mu_V^{h;\pm} \simeq \pm \frac{\alpha_V}{\pi\sqrt{3}} \delta\mu_V^{h;\pm}, \\ \delta\mu_{\tilde{\chi}}^{h;\pm} &= \frac{k\Omega T}{2\omega_h^\pm} \frac{A - s_V B}{\sigma_A^\omega - s_V \sigma_H^\omega} \delta\mu_V^{h;\pm} \simeq \pm \frac{s_V \alpha_V^4 \sqrt{3}}{4\pi^3} \delta\mu_V^{h;\pm}, \end{aligned} \quad (5.19)$$

where we displayed just the leading-order contribution in the degenerate limit. It can be seen that as $|\alpha_V| \rightarrow \infty$, a small excitation in $\delta\mu_V$ in either modes $\delta\mu_V^{h;\pm}$ will lead to excitations in $\delta\mu_{\tilde{\chi}}^{h;\pm}$ that are α_V^4 times larger, signalling the breakdown of the linear perturbations ansatz in the degenerate matter. Coming back to Fig. 5, considering the ratio $\alpha_V = \mu_V/T = 20$, our estimate above indicates $\delta\mu_{\tilde{\chi}}^{h;\pm}/\delta\mu_{V;0} \simeq 1117$ to leading order in α_V , which is in line with the results shown in the right panel of this figure.

The above discussion indicates that degenerate matter under rotation is unstable under small perturbations. A small excitation of the vector chemical potential induces huge excitations in the vector and helical chemical potentials, invalidating the linear regime ansatz of this analysis. One may question the physical soundness of these results. In our companion paper [26], we show that in a realistic plasma, the non-conservation of the helicity charge prevents the axial and helical mode amplitudes from growing, leading to perfectly reasonable propagation properties.

6 Summary and Conclusions

In our work, we challenge the traditional approach to chiral systems, which presumes that the chiral fluids are completely described only by the pair of the vector and axial local charges. We show that the inclusion of the helical degree of freedom enriches the hydrodynamic spectrum of the system. Since we explored various regimes of the vector-axial-helical triad of charges, it is worth summarizing the main features of our findings in a compact set of plots shown in Fig. 6.

In the high-temperature limit of low-density plasmas, where the temperature significantly exceeds the magnitude of any background chemical potential, we confirmed the existence of the Helical Vortical Wave, which corresponds to a gapless hydrodynamic excitation acting mainly in the helical and vector sectors of charge densities. In the next order in the series over the inverse temperature, this wave receives a slight admixture of the axial charge (3.22), indicating that all components of the fluid, represented by the vector, helical and axial charges, fluctuate coherently as the wave propagates as it is illustrated in Figs. 6(a) and 6(b). This next-order-correction gives us also a qualitatively

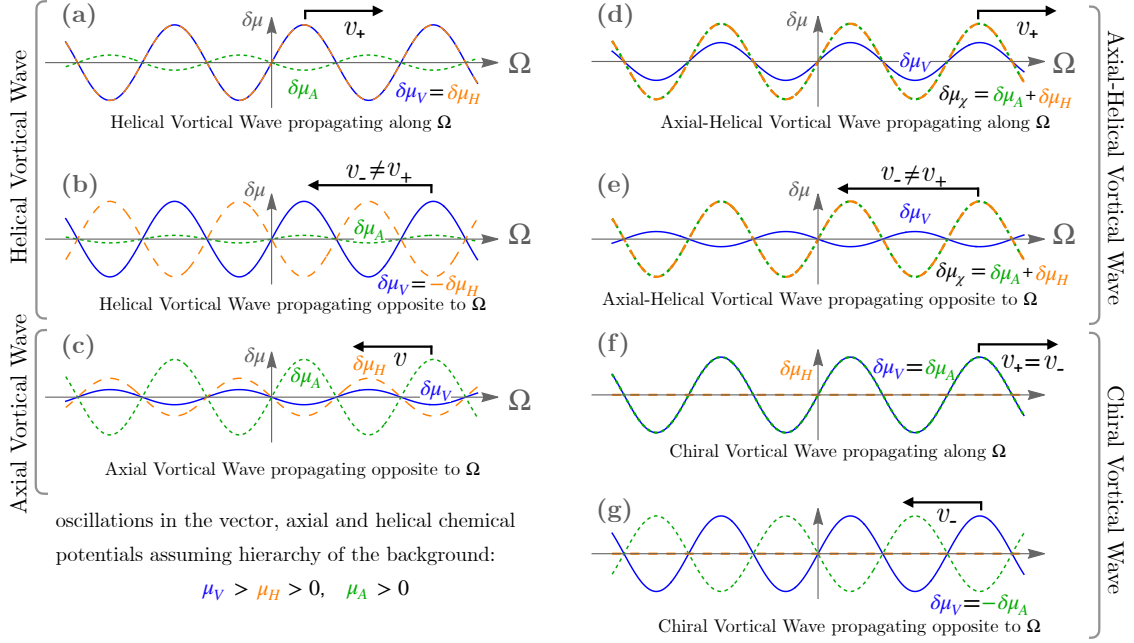


Figure 6: A summarising illustration of four classes of gapless hydrodynamic excitations discussed in the paper for the hierarchy $\mu_V > \mu_H > 0$ and $\mu_A > 0$ of the background chemical potentials. For simplicity, a gapless sinusoidal wave is shown only. A detailed description is given in the text.

unusual result implying the non-reciprocity of these hydrodynamic excitations: the helical vortical waves propagating along and opposite to the direction of vorticity possess different velocities (3.16).

Our approach also allows us to uncover yet another gapless wave in the system: the Axial Vortical Wave. According to Eq. (3.29), this wave propagates only in the presence of the axial chemical potential μ_A , since its velocity vanishes if $\mu_A = 0$. In the case when the other two charge densities are vanishing, the wave exhibits oscillations in the axial charge density, which propagate unidirectionally along (opposite to) the vorticity vector Ω for $\mu_A < 0$ ($\mu_A > 0$). In the presence of the background of vector (helical) charges, the purely axial wave is also accompanied by coherent fluctuations in axial and helical (or vector) charges (3.28), as it is illustrated in Fig. 6(c).

It is important to stress that the appearance of unidirectional transport in this simple homogeneous system is a fascinating and unexpected phenomenon that is distinct from the processes that usually occur in high-temperature plasmas. For example, in most classical acoustics and hydrodynamics, sound waves typically exhibit reciprocal propagation, meaning that the waves can travel forward and backwards along the same path without change in their propagation characteristics. On the contrary, the unidirectionality, seen from the point of view of ordinary acoustical waves, emerges as a result of the meticulously engineered breaking of time-reversal symmetry in the medium through which sound waves propagate. For example, in systems that break the time-reversal symmetry, sound waves can be en-

gineered to propagate in one direction while being significantly attenuated in the opposite direction [50].

The theoretical basis for unidirectional sound transport can, for example, be linked to the concept of topological insulators that represent materials that maintain propagating excitations only along their surface and not through their bulk [51]. Analogously, the unidirectional transport of sound waves has been realized through specific mechanisms, such as using exotic active materials with time-varying properties, creating asymmetric structures that induce directional bias, or employing magnetic fields in conjunction with magneto-acoustic materials [52].

On the practical level of acoustic (or, gapless, in a more generic sense) applications, the unidirectional transport includes acoustic diodes or rectifiers, which allow sound to pass through in one direction while blocking it in the opposite direction [53]. These devices could be used in noise reduction systems, acoustic logic devices, and improved ultrasonic imaging technologies [54]. Unidirectional sound propagation is an unusual phenomenon, and its appearance in a chiral plasma represents a fascinating, unexpected effect of an interplay of anomalous transport effects.

Coming back to the field-theoretical applications in chiral plasmas, we highlight our observation that at high densities, both the helical and the axial waves merge into a common hydrodynamic excitation, the Axial-Helical Vortical Wave. In this limit of the degenerate Dirac fluid, the magnitudes of helical and axial charge densities of the ensemble of particles are indistinguishable from each other since the helical and axial charges of a given particle (or anti-particle) are the same up to a sign. The Axial-Helical Vortical Wave maintains the property of non-reciprocity reflected in the velocities of its branches (5.12). Interestingly, there exists a critical temperature (5.14), at which one of the branches of this mixed wave stops propagating while the other one moves parallel to the direction of the vorticity vector. The mixed axial-helical vortical wave is illustrated in Figs. 6(d) and 6(e).

The discussion in this paper focussed on the simplified model where both the axial and the helical charges are conserved. As already discussed in Ref. [15], the helicity charge dissipates in a realistic plasma due to helicity-violation pair annihilation (HVPA) processes. Furthermore, the conservation of the axial charge is violated due to interactions via the axial anomaly [48]. The latter is dynamically relevant for the crossover region of finite-temperature QCD [23]. For the sake of completeness, we show in Figs. 6(f) and 6(g) the chiral vortical wave [2] which emerges in the limit where the helical degree of freedom is frozen due to strong relaxation [26]. We explore the consequences of the axial and helical charge non-conservation on the excitations spectrum revealed here in the companion paper [26].

Acknowledgments. This work is supported by the European Union - NextGenerationEU through grant No. 760079/23.05.2023, funded by the Romanian ministry of research, innovation and digitalization through Romania's National Recovery and Resilience Plan, call no. PNRR-III-C9-2022-I8. V.E.A. gratefully acknowledges partial support through a grant of the Ministry of Research, Innovation and Digitization, CNCS - UEFISCDI, project number PN-III-P1-1.1-TE-2021-1707, within PNCDI III.

References

- [1] D. E. Kharzeev and H.-U. Yee, *Chiral Magnetic Wave*, *Phys. Rev. D* **83** (2011) 085007 [[1012.6026](#)].
- [2] Y. Jiang, X.-G. Huang and J. Liao, *Chiral vortical wave and induced flavor charge transport in a rotating quark-gluon plasma*, *Phys. Rev. D* **92** (2015) 071501 [[1504.03201](#)].
- [3] G. M. Newman, *Anomalous hydrodynamics*, *JHEP* **01** (2006) 158 [[hep-ph/0511236](#)].
- [4] D. Kharzeev, K. Landsteiner, A. Schmitt and H.-U. Yee, eds., *Strongly Interacting Matter in Magnetic Fields*, vol. 871. Springer-Verlag, 2013, [10.1007/978-3-642-37305-3](#).
- [5] K. Fukushima, D. E. Kharzeev and H. J. Warringa, *The Chiral Magnetic Effect*, *Phys. Rev. D* **78** (2008) 074033 [[0808.3382](#)].
- [6] A. Vilenkin, *Equilibrium Parity Violating Current In A Magnetic Field*, *Phys. Rev. D* **22** (1980) 3080.
- [7] A. Y. Alekseev, V. V. Cheianov and J. Frohlich, *Universality of transport properties in equilibrium, Goldstone theorem and chiral anomaly*, *Phys. Rev. Lett.* **81** (1998) 3503 [[cond-mat/9803346](#)].
- [8] D. T. Son and A. R. Zhitnitsky, *Quantum anomalies in dense matter*, *Phys. Rev. D* **70** (2004) 074018 [[hep-ph/0405216](#)].
- [9] M. A. Metlitski and A. R. Zhitnitsky, *Anomalous axion interactions and topological currents in dense matter*, *Phys. Rev. D* **72** (2005) 045011 [[hep-ph/0505072](#)].
- [10] ALICE collaboration, *Probing the Chiral Magnetic Wave with charge-dependent flow measurements in Pb-Pb collisions at the LHC*, [2308.16123](#).
- [11] A. Vilenkin, *Parity Nonconservation and Rotating Black Holes*, *Phys. Rev. Lett.* **41** (1978) 1575.
- [12] A. Vilenkin, *Macroscopic Parity Violating Effects: Neutrino Fluxes From Rotating Black Holes And In Rotating Thermal Radiation*, *Phys. Rev. D* **20** (1979) 1807.
- [13] P. B. Pal, *Dirac, Majorana and Weyl fermions*, *Am. J. Phys.* **79** (2011) 485 [[1006.1718](#)].
- [14] V. E. Ambrus, *Helical massive fermions under rotation*, *JHEP* **08** (2020) 016 [[1912.09977](#)].
- [15] V. E. Ambrus and M. N. Chernodub, *Vortical effects in Dirac fluids with vector, chiral and helical charges*, *Eur. Phys. J. C* **83** (2023) 111 [[1912.11034](#)].
- [16] I. Gahramanov, T. Kalaydzhyan and I. Kirsch, *Anisotropic hydrodynamics, holography and the chiral magnetic effect*, *Phys. Rev. D* **85** (2012) 126013 [[1203.4259](#)].
- [17] N. Abbasi, A. Davody, K. Hejazi and Z. Rezaei, *Hydrodynamic Waves in an Anomalous Charged Fluid*, *Phys. Lett. B* **762** (2016) 23 [[1509.08878](#)].
- [18] N. Yamamoto, *Chiral Alfvén Wave in Anomalous Hydrodynamics*, *Phys. Rev. Lett.* **115** (2015) 141601 [[1505.05444](#)].
- [19] M. N. Chernodub, *Chiral Heat Wave and mixing of Magnetic, Vortical and Heat waves in chiral media*, *JHEP* **01** (2016) 100 [[1509.01245](#)].
- [20] N. Abbasi, D. Allahbakhshi, A. Davody and S. F. Taghavi, *Hydrodynamic excitations in hot QCD plasma*, *Phys. Rev. D* **96** (2017) 126002 [[1612.08614](#)].

- [21] T. Kalaydzhyan and E. Murchikova, *Thermal chiral vortical and magnetic waves: new excitation modes in chiral fluids*, *Nucl. Phys. B* **919** (2017) 173 [[1609.00024](#)].
- [22] N. Abbasi, K. Naderi and F. Taghinavaz, *Hydrodynamic Excitations from Chiral Kinetic Theory and the Hydrodynamic Frames*, *JHEP* **03** (2018) 191 [[1712.06175](#)].
- [23] M. Ruggieri, G. X. Peng and M. Chernodub, *Chiral Relaxation Time at the Crossover of Quantum Chromodynamics*, *Phys. Rev. D* **94** (2016) 054011 [[1606.03287](#)].
- [24] N. Astrakhantsev, V. V. Braguta, M. D’Elia, A. Y. Kotov, A. A. Nikolaev and F. Sanfilippo, *Lattice study of the electromagnetic conductivity of the quark-gluon plasma in an external magnetic field*, *Phys. Rev. D* **102** (2020) 054516 [[1910.08516](#)].
- [25] V. E. Ambrus and M. N. Chernodub, *Hyperon–anti-hyperon polarization asymmetry in relativistic heavy-ion collisions as an interplay between chiral and helical vortical effects*, *Eur. Phys. J. C* **82** (2022) 61 [[2010.05831](#)].
- [26] S. Morales-Tejera, V. E. Ambrus and M. Chernodub, *Vortical waves in a quantum fluid with vector, axial and helical charges: II. Dissipative effects, (a companion paper)*.
- [27] V. E. Ambrus and M. N. Chernodub, *Helical Separation Effect and helical heat transport for Dirac fermions*, [2307.14987](#).
- [28] X.-G. Huang, J. Liao, Q. Wang and X.-L. Xia, *Vorticity and Spin Polarization in Heavy Ion Collisions: Transport Models*, *Lect. Notes Phys.* **987** (2021) 281 [[2010.08937](#)].
- [29] J. Błoczyński, X.-G. Huang, X. Zhang and J. Liao, *Azimuthally fluctuating magnetic field and its impacts on observables in heavy-ion collisions*, *Physics Letters B* **718** (2013) 1529–1535.
- [30] K. Tuchin, *Initial value problem for magnetic fields in heavy ion collisions*, *Physical Review C* **93** (2016) .
- [31] U. Gürsoy, D. Kharzeev, E. Marcus, K. Rajagopal and C. Shen, *Charge-dependent flow induced by magnetic and electric fields in heavy ion collisions*, *Physical Review C* **98** (2018) .
- [32] W. Florkowski, A. Kumar and R. Ryblewski, *Relativistic hydrodynamics for spin-polarized fluids*, *Prog. Part. Nucl. Phys.* **108** (2019) 103709 [[1811.04409](#)].
- [33] F. Becattini, J. Liao and M. Lisa, *Strongly Interacting Matter Under Rotation: An Introduction*, *Lect. Notes Phys.* **987** (2021) 1 [[2102.00933](#)].
- [34] F. Becattini, *Spin and polarization: a new direction in relativistic heavy ion physics*, *Rept. Prog. Phys.* **85** (2022) 122301 [[2204.01144](#)].
- [35] STAR collaboration, *Global polarization measurement in Au+Au collisions*, *Phys. Rev. C* **76** (2007) 024915 [[0705.1691](#)].
- [36] STAR collaboration, *Global Λ hyperon polarization in nuclear collisions: evidence for the most vortical fluid*, *Nature* **548** (2017) 62 [[1701.06657](#)].
- [37] E. Nakano and T. Tatsumi, *Chiral symmetry and density wave in quark matter*, *Phys. Rev. D* **71** (2005) 114006 [[hep-ph/0411350](#)].
- [38] T. Tatsumi and E. Nakano, *Dual chiral density wave in quark matter*, [hep-ph/0408294](#).
- [39] S. M. A. Tabatabaee Mehr, *Chiral symmetry breaking and phase diagram of dual chiral density wave in a rotating quark matter*, *Phys. Rev. D* **108** (2023) 094042 [[2306.11753](#)].
- [40] H. M. Ghalati and N. Sadooghi, *Magnetic dual chiral density wave phase in rotating cold quark matter*, *Phys. Rev. D* **108** (2023) 054032 [[2306.04472](#)].

- [41] M. N. Chernodub and M. A. H. Vozmediano, *Chiral sound waves in strained Weyl semimetals*, *Phys. Rev. Res.* **1** (2019) 032040 [[1904.09113](#)].
- [42] F. Becattini, L. Bucciantini, E. Grossi and L. Tinti, *Local thermodynamical equilibrium and the beta frame for a quantum relativistic fluid*, *Eur. Phys. J. C* **75** (2015) 191 [[1403.6265](#)].
- [43] F. Becattini and E. Grossi, *Quantum corrections to the stress-energy tensor in thermodynamic equilibrium with acceleration*, *Phys. Rev. D* **92** (2015) 045037 [[1505.07760](#)].
- [44] V. E. Ambrus and E. Winstanley, *Exact Solutions in Quantum Field Theory Under Rotation*, in *Strongly Interacting Matter under Rotation*, F. Becattini, J. Liao and M. Lisa, eds., pp. 95–135, Springer, Cham, (8, 2019), [1908.10244](#), DOI.
- [45] V. E. Ambruş and M. N. Chernodub, *Vortical effects in Dirac fluids with vector, chiral and helical charges*, *Eur. Phys. J. C* **83** (2023) 111 [[1912.11034](#)].
- [46] K. Landsteiner, E. Megias and F. Pena-Benitez, *Gravitational Anomaly and Transport*, *Phys. Rev. Lett.* **107** (2011) 021601 [[1103.5006](#)].
- [47] C. Itzykson and J.-B. Zuber, *Quantum field theory*. Dover, 1980.
- [48] R. A. Bertlmann, *Anomalies in quantum field theory*. Clarendon Press, Oxford, UK, 1996.
- [49] M. Buzzegoli, *Thermodynamic equilibrium of massless fermions with vorticity, chirality and magnetic field*, Ph.D. thesis, Universita degli studi Firenze, 2020.
- [50] S. A. Cummer, J. Christensen and A. Alù, *Controlling sound with acoustic metamaterials*, *Nature Reviews Materials* **1** (2016) .
- [51] J. E. Moore, *The birth of topological insulators*, *Nature* **464** (2010) 194–198.
- [52] L. M. Nash, D. Kleckner, A. Read, V. Vitelli, A. M. Turner and W. T. M. Irvine, *Topological mechanics of gyroscopic metamaterials*, *Proceedings of the National Academy of Sciences* **112** (2015) 14495–14500.
- [53] R. Fleury, D. Sounas and A. Alù, *An invisible acoustic sensor based on parity-time symmetry*, *Nature Communications* **6** (2015) .
- [54] S. H. Mousavi, A. B. Khanikaev and Z. Wang, *Topologically protected elastic waves in phononic metamaterials*, *Nature Communications* **6** (2015) .